HIGHWAY RESEARCH RECORD

Number 218

Mechanical Properties of Plastic Concrete and Pavement Thickness Measurement

6 Reports

Subject Area

32 Cement and Concrete
33 Construction

HIGHWAY RESEARCH BOARD

DIVISION OF ENGINEERING NATIONAL RESEARCH COUNCIL
NATIONAL ACADEMY OF SCIENCES—NATIONAL ACADEMY OF ENGINEERING

Washington, D.C., 1968

Publication 1564

Price: $2.00

Available from

Highway Research Board
National Academy of Sciences
2101 Constitution Avenue
Washington, D.C. 20418

Department of Materials and Construction

R. L. Peyton, Chairman
State Highway Commission of Kansas, Topeka

HIGHWAY RESEARCH BOARD STAFF

R. E. Bollen and W. G. Gunderman

CONCRETE DIVISION

Bryant Mather, Chairman
U.S. Army Engineer Waterways Experiment Station
Jackson, Mississippi

COMMITTEE ON MECHANICAL PROPERTIES OF CONCRETE
(As of December 31, 1967)

Thomas W. Reichard, Chairman
National Bureau of Standards
Washington, D. C.

John D. Antrim
James W. Baldwin, Jr.
Irwin A. Benjamin
Karl H. Dunn
Frank L. Holman, Jr.
Clyde E. Kesler
D. A. Linger
V. M. Malhotra
Bryant Mather
Leonard J. Mitchell
Richard Alan Muenow
C. C. Oleson
R. E. Philleo
Sandor Popovics
Charles F. Scholer
V. R. Sturrup
E. A. Whitehurst

Foreword

The first four papers in this RECORD present data regarding some of the mechanical properties of fresh concrete that are of interest to concrete technologists as well as to users of concrete. The last two papers give an indication that the highway engineer's plea for a rapid, nondestructive method for determining pavement thickness may have been answered.

One of the most widely determined mechanical properties of fresh concrete is its consistency. The measured value of consistency is sometimes thought of as a measure of workability, while at other times it is thought of as a rough measure of the water content. It is well known that consistency, which can be determined by several methods, is not always a good indication of workability. In the first paper, Walz describes a simple "compacting ratio" method for determining consistency that may have some advantages as a measure of workability.

In the second paper, Popovics presents data which show that a known change in the water content of a concrete results in a predictable change in the consistency. Utilizing this finding, he proposes a method for calculating the needed adjustment in the water content for a required change in consistency.

In the third paper, Linger discusses some experiments showing the effect of several variables on the expansion of fresh concrete. Using aluminum powder as an expansion agent, he shows that the strength of the concrete from a particular mix is directly related to the volume of the voids produced.

Tyler, in the fourth paper, describes the length changes that occur in fresh and hardened concrete due to cement hydration and temperature changes. In describing the methods used in determining these data he also discloses some of the advantages and disadvantages in using acoustic strain gages.

The next paper, by Golis, reviews the performance of a pulse-echo type of ultrasonic instrument that has been used to measure the pavement thickness of newly constructed concrete pavements. He found that this instrument could rapidly measure the thickness of pavements to within 3 percent. This accuracy was attained even though the pulse velocity was assumed to be constant throughout a section of highway. Golis also recommends specific modifications to the equipment which would improve its performance.

In the last paper, Moore has utilized an adaptation of a widely accepted earth-resistivity test procedure in determining the thickness of concrete pavements with good precision. He also found that this technique can be useful in locating the steel in concrete slabs. Moore considers his work somewhat exploratory and suggests that further evaluation of the method be undertaken by some of the many state highway departments that are already using this equipment for subsurface explorations.

—T. W. Reichard

Contents

An Interpretation of the Results From Vibrating-Wire Strain Gauges in Fresh Concretes

R. G. TYLER, Road Research Laboratory, England

A program of tests concerning creep, shrinkage, and temperature movements in highway bridges is being conducted by the Bridges Section of the Design Division of the Road Research Laboratory. This paper describes the interpretation of the readings from acoustic strain gauges in fresh concrete, up to the time the heat of hydration is dissipated. Characteristics of the vibrating-wire gauge are described, together with the results of two laboratory experiments and three full-scale site investigations. The results show that usually expansions take place during the hydration of typical bridge concretes as used in the United Kingdom; these were manufactured from normal portland cement having water/cement ratios in the range 0.38 to 0.40.

Also discussed are the strain changes that occur on cooling during the dissipation of the heat of hydration in full-scale structures and cracking caused by differential strains on cooling. The effect of using a limestone aggregate having a low coefficient of expansion is shown; and it is demonstrated that cooling after hydration produces a self-straining set of forces within the concrete, the reinforcement being in tension to approximately 3,500 psi while the concrete is in compression.

•VIBRATING-WIRE strain gauges have been used extensively in investigations into creep, shrinkage, and temperature movements in concrete bridge structures. This paper is concerned with the interpretation of the readings from acoustic gauges in fresh concrete, up to the time the heat of hydration has dissipated. The work is necessary to establish a true zero for the gauge readings, i.e., the time from which readings taken to obtain an estimate of creep and shrinkage became meaningful. The work has also shed further light on the cause of early shrinkage cracking.

VIBRATING-WIRE STRAIN GAUGE

General

The vibrating-wire strain gauge has been developed in several European countries for measuring strains in structures, as a surface gauge for both steel and concrete structures, and as a buried gauge for concrete structures. Its main advantage, compared with other strain gauges, is its stability over long periods of time, which makes it ideal for measuring creep and shrinkage movements in concrete bridges. The gauge and readout equipment are commercially available in Europe (1, 2).

Essentially, the gauge consists of a wire stretched between two anchorage points. A change in the distance between the anchorage points, caused by strains in the structure, changes the natural frequency of vibration of the wire. An electromagnet at the center plucks the wire and transmits the frequency to a comparator. This instrument

Paper sponsored by Committee on Mechanical Properties of Concrete and presented at the 47th Annual Meeting.

compares the frequency with a standard frequency (e.g., from a tuning fork or quartz crystal) and indicates either the frequency of vibration, or the time required to complete a given number of cycles, i.e., the inverse of the frequency. Strain in the wire is given by

$$\epsilon_w = Kf^2$$

where f = frequency of vibration. The constant K is known as the gauge factor and is given approximately by

$$K = \frac{4l^2\rho}{Eg}$$

where

- l = length of vibrating wire,
- ρ = density of wire,
- E = modulus of electicity of wire, and
- g = acceleration due to gravity.

In practice, K is normally determined experimentally, mainly because the vibrating length of the wire may not be the same as the effective length of the strained concrete between the flanges. When used to measure strains in a structure:

ϵ = movement per unit length in structure caused by loading, shrinkage, or other effect
= $K (f_1^2 - f_2^2)$

where f_1 = frequency of vibration of wire in cycles per sec at time zero; and f_2 = frequency of vibration of wire after application of load, shrinkage, or other effect.

RRL Buried Gauge

Description—In the current program of tests on concrete bridges, gauges of the RRL type have been used (3). They were developed initially with a ¼-in. diameter "perspex" (a transparent acrylic plastic) tube for low stiffness in measuring tensile strains in concrete (Fig. 1). Subsequently, for work on prestressed bridges a ¼-in. stainless steel tube 0.010 in. thick has been used, principally to make the gauge less liable to damage; otherwise the gauge is identical to that shown. For both types of

Figure 1. RRL acoustic strain gauge with transparent acrylic plastic barrel.

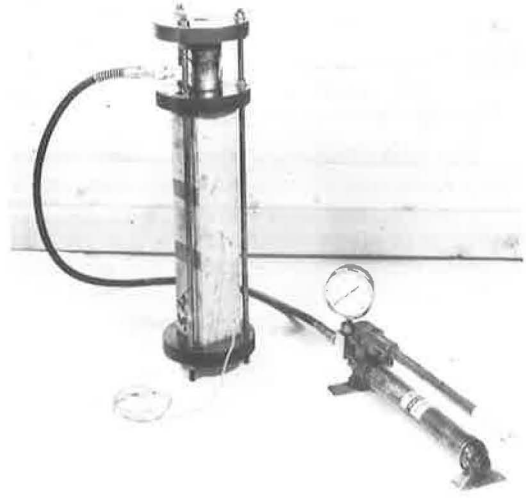

Figure 2. RRL creep rig.

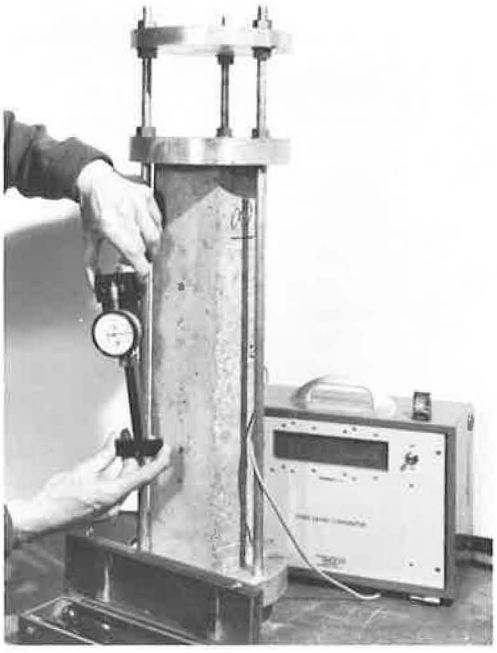

Figure 3. Demec gauge in use for the measurement of surface strain on a concrete specimen.

gauge the tubes are rigidly connected to the end flanges so that in straining the wire the tubes must also be strained. A silver-plated 0.010-in. diameter piano wire is used as the vibrating wire and the gauge length is 5½ in. The wire may be heat-treated to avoid creep at elevated temperatures (4); but creep at normal atmospheric temperatures is small, provided that the gauge is tensioned a few days prior to insertion in the structure.

Gauge Factor—The gauge factor for the RRL gauge has been determined by embedding gauges at the center of standard concrete specimens 20 by 4 by 4 in., which are loaded axially in creep rigs (Fig. 2). The mean strain, as recorded by a 12-in. or 8-in. "demec" gauge (demountable mechanical gauge, Fig. 3) on opposite sides of the prism, is compared with the change of frequency recorded by the acoustic gauge at the center. Experiments have been carried out using several batches of specimens, and the mean value of K for gauges having both plastic and steel tubes has been found to be 3.0×10^{-9}, i.e., $\epsilon = 3.0 \times 10^{-9} (f_1^2 - f_2^2)$ in./in.

The scatter of the gauge factor for individual gauges is difficult to determine by this method because errors in the demec gauge readings are included in the observations, and this instrument, which is hand-held, is susceptible to operator error. From the viewpoint of carrying out the measurements, the least sensitive of the portable equipment used for measuring the frequency of vibration is capable of resolving to within $\pm 3 \times 10^{-6}$ in./in. in the range 1,000 to 600 cycles per sec. However, when using a variety of equipment for the same test, it is desirable to check their comparative accuracy by using a standard reference tuning fork because temperature changes can cause a small drift of the built-in reference units.

Coefficient of Expansion for Vibrating Wire—The value for the coefficient of expansion of 0.010-in. thick silver-plated piano wire is $12.0 (\pm 0.5) \times 10^{-6}$ per deg C. This is an important characteristic of the gauge, since it roughly corresponds with the coefficient of expansion of gravel and quartzite aggregate concretes (6) that form a large proportion of the concretes manufactured in the United Kingdom, and also to the measured values of coefficient of expansion of bridges in Southern England (7, 8). Thus temperature changes cause the wire to expand with the concrete and, in general, only elastic strains, creep, and shrinkage are recorded by the gauge.

LABORATORY INVESTIGATIONS

Characteristics of Various Types of Acoustic Gauge When Embedded In Fresh Concrete

Gauges of three different types were embedded in a block of concrete 10 by 10 by 9 in. (Figs. 4 and 5) and readings were taken immediately after casting, initially at hourly intervals and later at less frequent intervals.

The block was insulated on its sides by 1-in. thick sheets of expanded polystyrene, to simulate the thermal conditions found in a large concrete element during hydration of the cement.

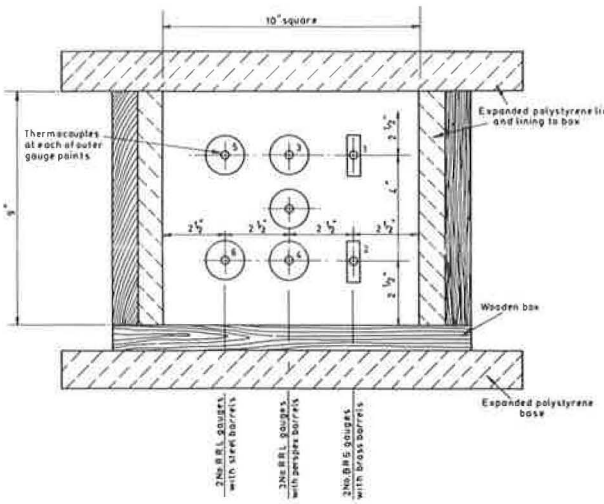

Figure 4. Details of concrete block.

Description of Installation—The three different types of gauges were (a) RRL gauge with steel barrel, (b) RRL gauge with plastic barrel, and (c) BRS gauge (9). The BRS gauge was developed by the Building Research Station, United Kingdom, and has an identical vibrating-wire element to the RRL gauge. However, a pillar is used as an end anchorage instead of a circular flange, with a different clamping method for the wire; a brass tube is employed.

Two RRL steel, two BRS, and three plastic RRL gauges were used; three of the latter were provided to allow for the possibility of one gauge being damaged during vibration of the concrete, the plastic tubes being more vulnerable to damage than the metal ones. Six thermocouples were also buried at the outer gauge positions in order to measure temperatures during setting. In addition, two 20 by 4 by 4-in. control specimens were cast in cast-iron molds that were not insulated. One of the molds was lined at the bottom and sides with $\frac{1}{4}$-in. thick corrugated cardboard to allow for free expansion of the concrete. Two RRL steel-barreled gauges were cast into each of the control specimens along the longitudinal axis of the specimens, together with thermocouples.

Concrete Mix—A mix similar to that employed for prestressed concrete of the river spans of the Medway Bridge (10) was used, but without plasticizer, i.e.:

1. 1 part normal portland cement,
2. 1 part flint-gravel sand,
3. 0.68 part $\frac{3}{16}$ - $\frac{3}{8}$-in. flint-gravel aggregate,
4. 2.32 part $\frac{3}{8}$ - $\frac{3}{4}$-in. flint-gravel aggregate, and
5. 0.4 water-cement ratio.

The mold was vibrated on a vibrating table.

Results—The graphs summarize the recorded strains and temperatures in the block (Fig. 6) and strains in the control specimens (Fig. 7). In the block, the temperature was found to be almost uniform in the region of the gauges and is plotted in the top curve (Fig. 6). A temperature rise of 22 C from the ambient laboratory temperature of approximately 15 to 37 C is indicated over the first 20 hours, followed by a gradual fall over the next four days. On the other hand, the temperature of the control specimens remained almost constant at the ambient laboratory temperature of 15 C.

All the strain gauges recorded an expansion during the temperature rise, but of differing amounts. In the block, the range of expansion up to 20 hours was from about 171×10^{-6} in./in. in one of

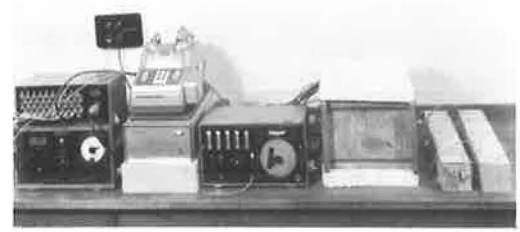

Figure 5. Data logger, insulated block, and demolded control specimens.

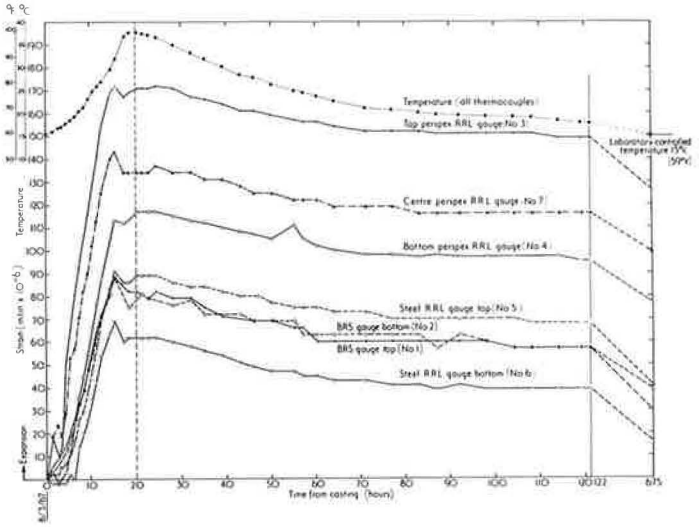

Figure 6. Movement and temperature in concrete block.

the plastic gauges at the top of the group to 62 x 10^{-6} in./in. in a steel-barreled gauge at the bottom (Table 1).

In the control specimens the peak of expansion occurred at about 40 hours and the range was from 168 x 10^{-6} in./in. in one of the gauges in the lined specimen to 106 x 10^{-6} in./in. in the same specimen (Table 2).

In the block, the plastic-barreled gauges showed the greatest increase, while the steel- and brass-barreled gauges were grouped roughly together. In addition, the plastic and steel gauges showed greater expansion at the top of the block than at the bottom.

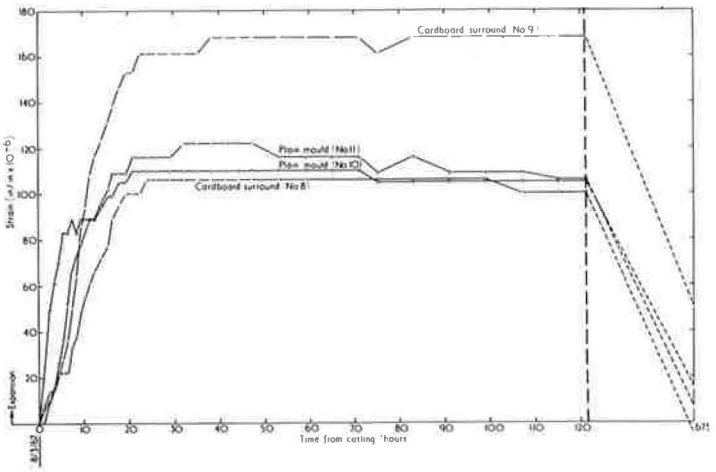

Figure 7. Movement in 20 by 4 by 4-in. control specimens.

TABLE 1
GAUGE TESTS

Time	RRL Gauges					BRS Gauges	
	Plastic-Barreled			Steel-Barreled			
	3*	7*	4*	5*	6*	1*	2*
Expansion 20 hr after casting	171	134	117	89	62	79	82
Arbitrary zero at 20 hr	0	0	0	0	0	0	0
120 hr	-22	-18	-22	-21	-23	-25	-22
28 days	-45	-35	-40	-42	-46	-30	-39
5 months	-111	-99	-100	-97	-119	-119	-109

*Gauge No.—3, 5, 1, top; 7, middle; and 4, 6, 2, bottom

NOTE: Shrinkage (in./in. x 10^{-6}) used where applicable.

TABLE 2
GAUGE TESTS

Time	Steel-Barreled RRL Gauges			
	Cardboard Surround		Plain Mold	
	8*	9*	10*	11*
Expansion 40 hr after casting	106	168	111	122
Arbitrary zero at 40 hr	0	0	0	0
120 hr, specimen in mold	-6	0	-5	-16
28 days, specimen demolded	-111	-118	-95	-116
5 months	-246	-264	-234	-190

*Gauge No.

After the maximum temperature had been reached in this block, the strain readings dropped by an amount which is approximately the same for all the gauges (Table 1); the block was not demolded. This was also approximately true for the control specimens (Table 2). The readings are greater than those for the block because of the greater size of the block cross section and because the small specimens were demolded.

Discussion—During hydration, an expansion was indicated by all gauges, both in the block and in the control specimens, but by differing amounts. Since there was a negligible temperature rise in the control specimens, it can be concluded that the expansion was the result of volume change during setting but not directly the result of temperature rise. The phenomenon of expansion in setting has been recorded by other workers (4, 11, 12). Browne and McCurrich (4) established that the amount of movement indicated by a gauge depends on its stiffness in resisting the movement of the concrete. This was expressed as a "response factor," i.e., the force per unit area to produce unit strain in the gauge. While the plastic gauge has the lowest response factor, it also has a high coefficient of expansion (80 x 10^{-6} per deg C), so that when a temperature rise occurs the expansion of the gauge assists the movement and possibly exaggerates the readings. One question that arises in this particular instance is whether the expansion in the plane of the plastic gauges, i.e., in a vertical plane at the center of the block, is greater than the expansion nearer the edges in the plane of the other gauges. The next experiment described indicates that this is not likely.

The amount of expansion also appears to depend on the stiffness of the mold or on pressures within the concrete, greater movements occurring near the top of the wooden mold used for the block. It is surprising that the cast-iron mold used for the unlined control specimen moved at all, but because the total expansion for 171 microstrain on 20 in. is only about 0.003 in., presumably this amount of movement could be found at the end fittings.

Figure 8. River Aire Bridge—south cantilever.

Results from the block show that once the concrete has set, its stiffness is so great that the effect of different types of gauge barrel is negligible. Thus subsequent shrinkage readings are the same for all three types. It is apparent that the maximum volume condition of concrete is reached when the temperature of hydration is at its peak. Thereafter the concrete shrinks through moisture loss and also

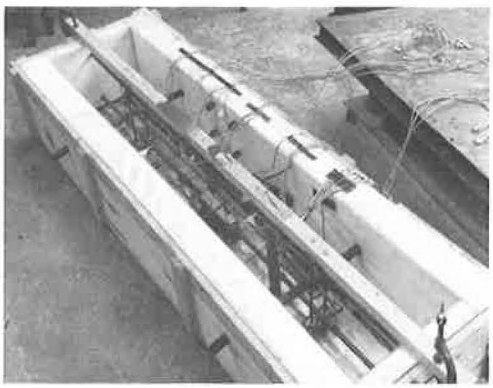

Figure 9. Mold for simulated-deck experiment, River Aire Bridge.

contracts due to the thermal drop. Where the coefficient of expanison of the concretes is different, this has to be allowed for in calculations of shrinkage.

Experiment to Determine Behavior of Deck Sections of River Aire Bridge Immediately After Casting

The River Aire Bridge at Ferrybridge, Yorkshire, was completed by the West Riding of Yorkshire in 1967 (Fig. 8). It is of double cantilever construction with a 280-ft main span between piers and was built by the cantilever method of construction to a central shear hinge in the manner of many European bridges. A computer program was used to control the construction levels to allow for deflections arising from creep and shrinkage over 10 years. The following experiment was carried out in 1965 to determine the initial state of stress of the reinforcement immediately after casting because, at the time, it was felt that this might contribute to the strain behavior of the structure. This supposition arose because of an anomaly in the results from the Medway Bridge investigation (13) when an explanation was sought for the fact that the total creep, shrinkage, and elastic strain in the bottom slab, which was loaded to 600 psi, was found to be little greater than the shrinkage of 28 by 6 by 6-in. control specimens that were housed within the box girders of the bridge and waterproofed to give approximately the same surface area/volume ratio.

Description of Experiment—A section representative of the deck slab of the River Aire Bridge, 13¾ in. wide by 12 in. deep by 5 ft 6 in. long (Fig. 9), was cast, the width being equal to the spacing between the ⅝-in. diameter high-tensile indented reinforcing bars in the top and bottom mats of the slab, two of which were included, while the depth was the actual slab depth on the bridge. The length was thought sufficient to give bond on the reinforcing bar, and thermal continuity in the bridge slab was simulated

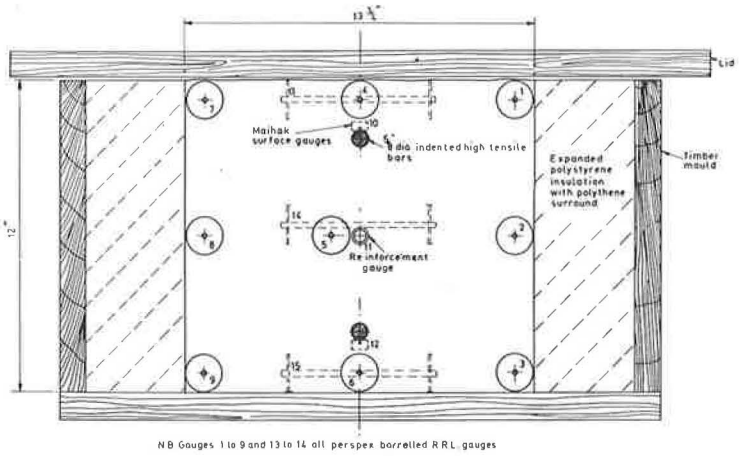

Figure 10. Cross section showing gauge positions, River Aire Bridge experiment.

Figure 11. Reinforcement acoustic gauge.

by a 4-in. thick expanded polystyrene lining to the walls of the mold, which was covered in a layer of polythene.

The disposition of the vibrating-wire gauges is shown in the cross section (Fig. 10), the gauges being near to the center of the length of the specimen but staggered along the length where necessary. A dozen perspex-barreled gauges were used, two of which failed to operate after the vibration of the concrete. In addition, a Maihak surface vibrating-wire gauge was fitted on one side of each reinforcing bar; these were contained in small hardboard boxes surrounding the bar to prevent the ingress of the wet concrete. Also an experimental type of vibrating-wire gauge (Fig. 11) known as a tubular or "reinforcement" gauge was cast into the center of the block. This gauge was developed at the Laboratory in order to obtain an estimate of the stresses in reinforcement without instrumenting it. It is made from a long steel tube, $\frac{1}{2}$-in. diameter, and 20 SWG (0.036 in.) thick, and is of constant cross section apart from the section at the center, where a plucking coil is inserted through the wall of the tube. A standard vibrating-wire element $5\frac{1}{2}$ in. long is included at its center, and the tube behaves as a hollow reinforcing bar. Experiments are still being conducted with the gauge, and while these suggest that a 3-ft tube is sufficient to give bond, a 4-ft tube was used in this experiment. The cross-sectional area of the tube is 0.052 sq in., which is slightly greater than a normal $\frac{1}{4}$-in. diameter reinforcing bar.

Concrete Mix—Aggregates were brought into the Laboratory from the bridge site for the tests and the proportions were as follows:

1. 1 part normal portland cement,
2. 1.43 parts quartzite river sand,

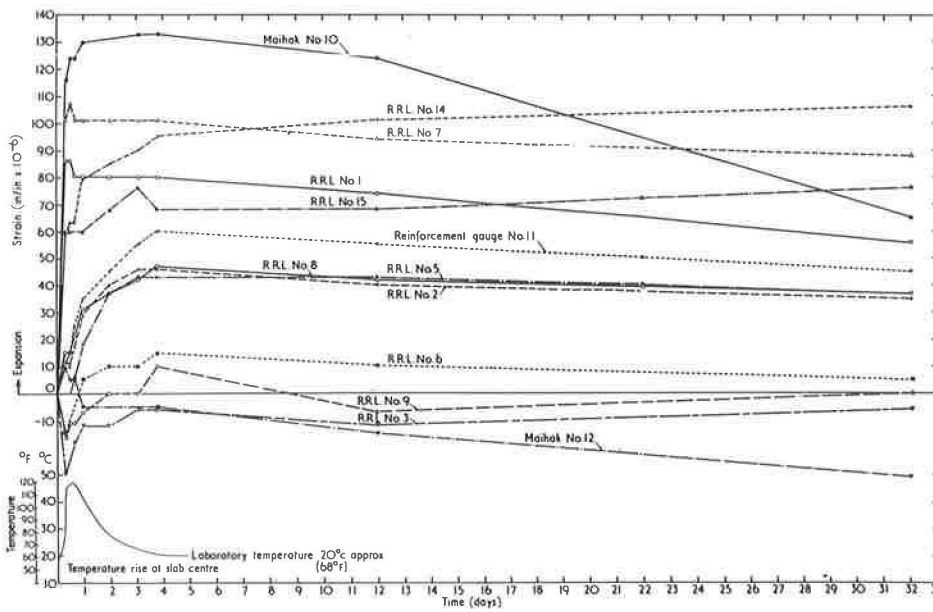

Figure 12. Strains and temperature variations for simulated deck slab, River Aire Bridge.

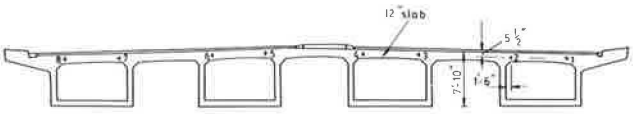

Figure 13. Cross section showing gauge positions on River Aire Bridge.

3. 0.91 parts $\frac{3}{8}$-in. quartzite river gravel,
4. 1.46 parts $\frac{3}{4}$-in. quartzite river gravel,
5. Water/cement ratio 0.39,
6. Slump 1 in., and
7. Compacting factor 0.84.

The mold was vibrated on a vibrating table.

Results—The results follow a similar pattern to those obtained in the experiment previously described.

The graph (Fig. 12) shows that gauges indicated expansions of zero up to 130×10^{-6} in./in. during the hydration of the cement. In the longitudinal direction maximum values occurred at the top of the molds, while transversely maximum values occurred at the bottom, adjacent to the lower shuttering. The values of strain for the steel reinforcement and the reinforcement gauge follow the same pattern as the less-rigid perspex gauges, although the possibility arises that the rise in strain in the upper steel bar may have been exaggerated as it was only instrumented on one side. The temperature rise at the center of the mold was 28 C. The peak temperature at the surface of the concrete just below the lid was about 4 C lower than that at the center of the mold, and other temperatures were intermediate in value, showing that there was very little temperature gradient over the depth of the concrete.

Discussion—From the results it would appear that the expansions which occur during setting load the reinforcement in tension, principally depending on its position in the concrete; e.g., the stress which occurs in the reinforcement gauge at the center of the slab is given by

$$\text{Stress} = 60 \times 10^{-6} \times 30 \times 10^{+6}$$
$$= 1,800 \text{ psi}$$

This is the peak stress at the center of the slab after 4 days; thereafter, shrinkage took place that would reduce and eventually neutralize the tensile stress. Note that very little shrinkage had occurred in the slabs up to 32 days, even though it was in a comparatively dry laboratory atmosphere. This may be explained by the size of the block and the fact that in order to maintain the waterproofing on its sides, it was not demolded. The apparently rapid loss in strain in the upper and lower reinforcement bars (Maihak gauges No. 10 and 12) was later found to be caused by corrosion of the wires of gauges that had been used on a previous investigation outside and stored for some years. This caused a steady creep loss in the wire. This trouble does not, however, occur with buried gauges that are sealed.

By way of comparison, the average shrinkage loss of all the gauges in the slab after two years was 100×10^{-6} in./in. from the peak of hydration. The slab had not been demolded and was stored in a dry unheated hangar. A control specimen 28 by 6 by 6 in. had shrunk 130×10^{-6} in./in. over the same period of time. This had been demolded.

As a result of this experiment, it was felt that it would not be worthwhile to make any allowance for the initial tensile stress in the reinforcement in the computer program because the stress level was not high, and further experimentation would be needed to establish the effect of casting the deck slab on the full scale.

SITE INVESTIGATIONS

Recorded Movements in Fresh Concrete for a Section of the River Aire Bridge

Opportunity was taken during the construction of the River Aire Bridge to check the readings obtained in acoustic gauges during the casting of a typical section of the bridge, some two years after the experiment previously described was completed. Steel-bar barreled gauges of the standard RRL type were buried in the top slab (Fig. 13). A

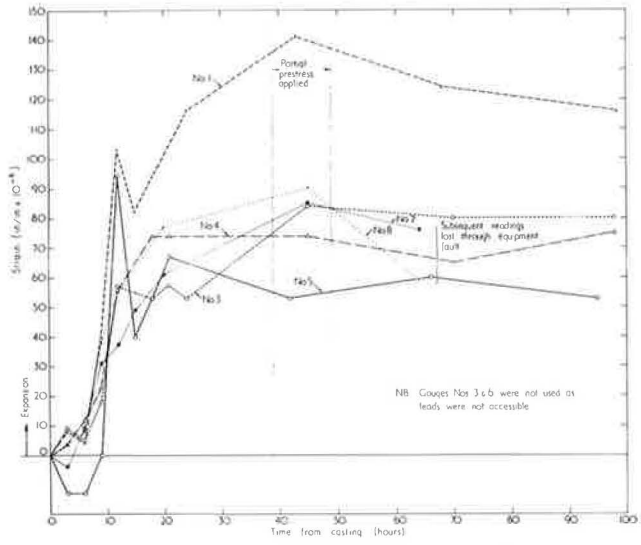

Figure 14. Strains after casting deck slab, River Aire Bridge.

partial prestress was applied to the bridge at 39 hours using a small proportion of the prestressing bars.

Concrete Mix—The concrete mix had been modified since the tests in 1965 and was as follows:

1. 1 part normal portland cement,
2. 1.14 parts quartzite river sand,
3. 1.07 parts $\frac{3}{8}$-in. quartzite river aggregate,
4. 1.60 parts $\frac{3}{4}$-in. quartzite river aggregate,
5. "Febflow" plasticizer at the rate of 16 oz per $\frac{1}{2}$ cu yd of mix,

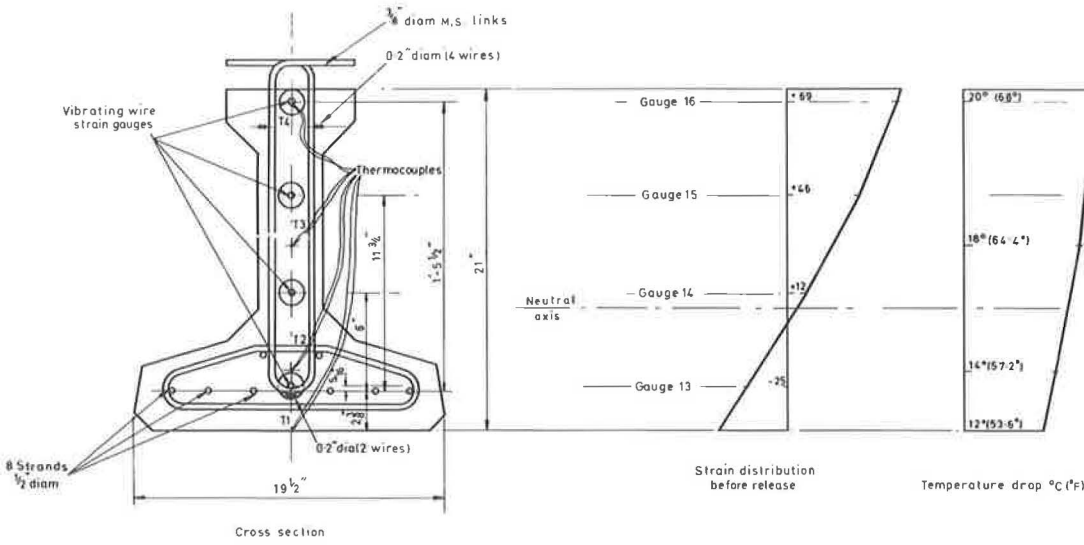

Figure 15. Strain and temperature changes in precast beams on cooling.

6. Slump 2 in.,
7. Compacting factor 0.94, and
8. Average concrete strength at 28 days, 9,000 psi.

Vibration was carried out by using poker vibrators.

Results—The graphs (Fig. 14) show that expansions in the range 130 - 50 x 10^{-6} in./in. were recorded up to the time the partial prestress of 54 lb/in.^{2} was applied to the top slab, which caused slight reductions in the recorded tensile strains. No temperatures were measured, but it is probable that the temperature increases were about the same as those recorded during the laboratory experiment.

Discussion—The results show a similar pattern to those recorded in the laboratory experiment with maximum values of expansion approximately 130 x 10^{-6} in./in.

Behavior of Gauges During Casting of Prestressed Beams Manufactured By the Long-Line Method

A further opportunity was obtained to check strain changes that occurred on casting during the manufacture of prestressed beams at the factory of Concrete (Southern) Ltd., which were to be the subject of other tests at the laboratory. The beams were standard Prestressed Concrete Development Group beams of I section (Fig. 15), 35 ft 3 in. long and 21 in. deep. Steel molds were used for the beams, which were cast over a heated floor maintained at about 55 C.

Investigation Method—Four steel-barreled gauges were strapped by soft iron wire to the stirrups of the beam in the positions indicated in Figure 15. Thermocouples were also buried in the concrete over the depth of the beam as shown. The concrete was cast at 5 p.m. on the first day when the molds were covered with a tarpaulin, which was removed at 7 a.m. the following morning immediately before stripping the molds. Between 7 a.m. and 1 p.m. devices were stuck to the beams to give an indication of their deflection on release. This caused a delay in release which was outside the normal works procedure, as usually the long-line prestressing forces would

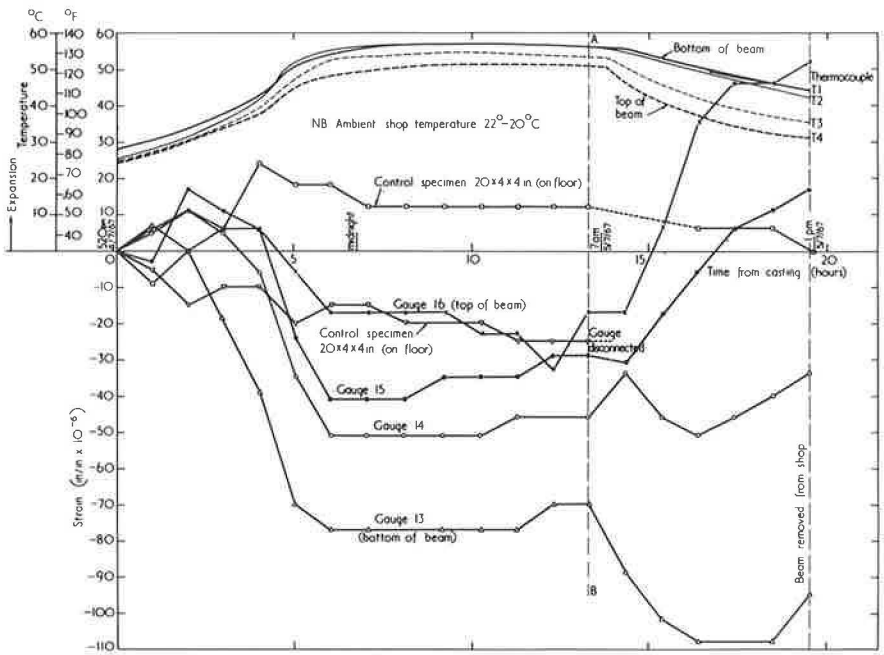

Figure 16. Strain and temperature records for precast beams.

have been released immediately after the removal of the covers. Strain and temperature readings were taken continuously for 24 hours using automatic equipment.

Concrete Mix—The concrete mix was as follows:

1. 1 part Ferrocrete rapid-hardening portland cement,
2. 1.01 part Thames Valley flint sand,
3. 0.53 part Thames Valley $^3/_8$-in. flint gravel aggregate,
4. 1.97 part Thames Valley $^3/_4$-in. flint gravel aggregate,
5. Water/cement ratio 0.38,
6. $^1/_4$ pint plasticizer (Sealoplaz) per cwt cement,
7. 1 in. slump, and
8. Average 28 days strength 8170 lb/sq in.

Vibration was carried out by means of poker vibrations.

Results—The temperatures measured at the top in the beam are shown plotted in Figure 16. These show that even with the tarpaulins on, the beams were hotter adjacent to the floor, the difference in temperature between the top and bottom being about 6 C throughout the night prior to removing the covers at 7:00 a.m. Thereafter, the tops of the beams cooled and the temperature difference increased to a maximum value of about 13 C at noon.

The strain gauge results showed that there was longitudinal shrinkage throughout the depth of the beam during setting, the greatest value of shrinkage occurring at the bottom of the beam. This movement had, however, ceased by midnight on the day of casting, and conditions remained constant during the night up to the time the covers were removed. After the covers were removed, however, and the molds stripped, a strain gradient built up, caused by the differential cooling of the top of the beam relative to the bottom. The strain gradient for 1 p.m. just prior to release is shown in Figure 15 for zeros taken at 6:40 a.m., corresponding to the line AB on the graph (Fig. 16), the values of strain being as given in Table 3.

Separate tests gave the modulus of elasticity of the concrete as $4.5 \times 10^{+6}$ lb/sq in. at 1 p.m. For a strain of 69×10^{-6} in./in. and a section modulus of 565 in.^{3} at the beam top, the indicated thermal moment was

$$\text{Moment} = 69 \times 10^{-6} \times 4.5 \times 10^{+6} \times 565$$
$$= 175{,}000 \text{ lb-in.}$$

This is a true value of moment since the coefficient of expansion of a Thames gravel aggregate concrete and the wire of the gauge are roughly equal. Thus while simple expansions and contractions arising from temperature changes cause little variation in the gauge reading, the gauge indicates strains caused by restraints to thermal movement; e.g., in this instance, the gauge at the top of the beam cooled with the concrete, but was held roughly to its original length by the restraint imposed by the prestressing cables holding the beams down to the floor. A true value of tensile strain was therefore recorded.

At noon, cracks were detected in two of the beams running from the top down to the bottom of the web, corresponding to the position of the tensile zone of the diagram (Fig. 15). These closed up when the prestress was released at 1 p.m. The cracks would not have occurred with the normal works procedure, when the beams are released about one hour after stripping the molds.

TABLE 3
VALUES OF STRAIN

Gauge No.	Reading		Values to Arbitrary Zero, 6:40 a.m.
	6:40 a.m.	1 p.m.	
13 (bottom of beam)	-70	-95	-25
14	-46	-34	+12
15	-29	+17	+46
16 (top of beam)	-17	+52	+69

NOTE: Strain (in./in. $\times 10^{-6}$) used where applicable.

Discussion—The results underline a characteristic of this acoustic gauge, viz., that it will indicate directly strains caused by thermal restraint

Figure 17. Mancunian Way elevated road.

when the coefficient of expansion of the steel wire is roughly the same as that of the concrete as for the gravel and quartzite aggregates. Where other aggregates are used, e.g., limestone, adjustment to the readings would be required.

This is a useful characteristic when investigating the cracking which arises soon after casting; it is usually termed shrinkage cracking. Experiment indicates that early shrinkage caused by moisture loss and carbonization is, in fact, small in full-scale structures in the temperate climate of the United Kingdom. Thus cracking in the first week after casting is more likely to be caused by thermal differences than by moisture loss, in particular by cooling of the outside surface of a section relative to the inside as occurred for the precast beams. It has already been shown for the Medway Bridge that temperature drops of up to 45 C occurred in the deck structure, for which the associated contraction was about 500×10^{-6} in./in. In addition, the more exposed parts of the deck slab midway between the webs reached a lower peak temperature than the thicker parts of the webs, and differences of up to 30 C have been recorded (13, 14). This represents a differential strain in cooling of approximately 360×10^{-6} in./in., which would cause cracking where secondary reinforcement is insufficient. In this instance, cracking occurred at an early age when the difference in temperature promoted by temperature drop was only 7 C and the associated value of tensile strain was 70×10^{-6} in./in.

Behavior of Gauges When Cast Into a Section of the Mancunian Way

A full-scale investigation has also been carried out into the movements occurring in the Mancunian Way, an overhead road in Manchester completed in 1967 (Fig. 17). In this investigation steel-barreled gauges were used. Some were briquetted in small concrete blocks 6 by 2 by 2 in. prior to casting and others were not; the purpose of this was to ascertain whether an unbriquetted gauge was sufficiently robust to withstand the pouring of concrete and vibration by poker vibrators when no special care was taken.

Site Procedure—The structure was factory cast in 10-ft sections which were later prestressed together on site. Gauges were tied to the secondary reinforcement in a typical section at the points indicated in the cross section (Figs. 18 and 19). Readings

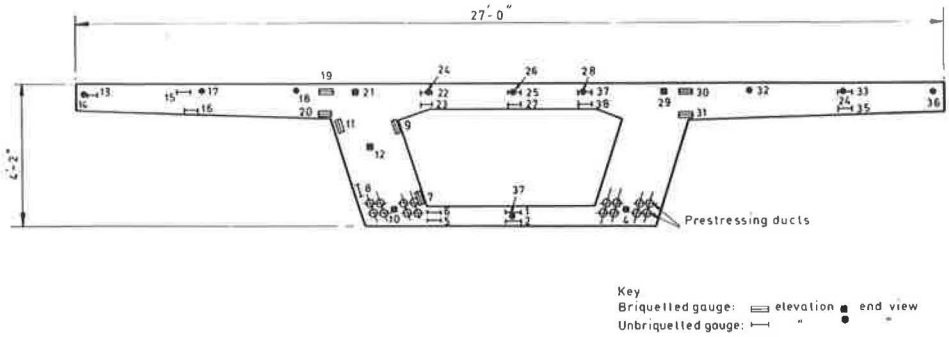

Figure 18. Gauge positions in Mancunian Way unit.

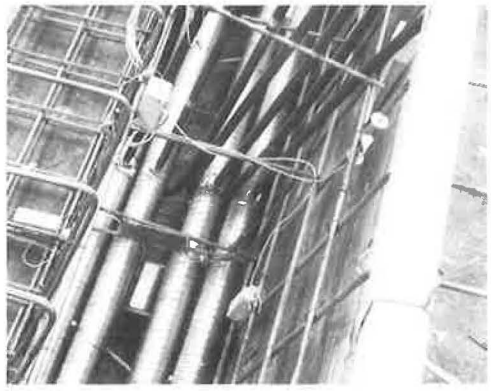

Figure 19 Biquetted and bare gauges in web of Mancunian Way precast unit (the internal shuttering has not been placed).

were taken on all gauges after they had been fixed in the structure. The concrete was poured in one operation and the shuttering was struck one day after casting, but it was not possible to take further readings until one week later.

Concrete Mix—This was as follows:

1. 1 part ordinary portland cement,
2. 0.71 part river sand,
3. 0.95 part $\frac{3}{8}$-in. crushed limestone,
4. 1.89 part $\frac{3}{4}$-in. crushed limestone,
5. 0.38 water/cement ratio,
6. Slump 2 in.,
7. Compacting factor 0.88, and
8. 1 pint of plasticizer per 12 cu ft of mix.

For the briquetting of the gauges, a similar mix was used, but with $\frac{3}{8}$-in. gravel aggregate instead of the $\frac{3}{4}$ to $\frac{3}{16}$ in. sizes in the main mix. The briquettes were about one week old at the time of tying into the structure and had been stored in the laboratory after being cured for two days under polythene. The results are given in Table 4.

Again there is a tendency for the greatest recorded expansions to occur near the top of the mold. The maximum value of 238 microstrain occurred in gauge 19 at the surface of the unit, while the minimum value of -12 microstrain occurred in the base slab. The results for eight companion specimens 20 by 4 by 4 in., which were kept exposed outside but not waterproofed at the laboratory and having steel-barreled gauges at their centers, are given in Table 5. Unfortunately no intermediate readings were taken, but measurements taken on other companion specimens for the same structure indicate a steady shrinkage from immediately after casting.

TABLE 4

BRIQUETTING OF GAUGES

Briquetted Gauges				Unbriquetted Gauges			
Gauge No.	5/10/66 Before Casting: Gauges in Position	5/17/66 Six Days After Striking Shuttering	9/7/66 On Site, Just Prior to Prestressing	Gauge No.	10/7/66 Before Casting: Gauges in Position	5/17/66 Six Days After Striking Shuttering	9/7/66 On Site, Just Prior to Prestressing
1	0	+87	+4	2	Gauge lead defective		
4	0	+113	+49	3	0	+40	-13
6	0	+22	-8	5	0	-12	-74
8	0	+179	+139	7	0	+83	+84
9	0	+161	+114	11	0	+122	+29
10	0	+141	+60	13	0	+132	+145
12	0	+188	+137	14	0	+75	+70
19	0	+238	+250	15	0	+155	+201
20	0	+135	+30	16	0	+141	+64
21	0	+202	+177	17	0	+159	+164
29	0	+106	+146	18	0	+146	+127
30	0	+205	+234	22	0	+133	+112
31	0	+107	+60	23	0	+106	+189
Average expansion		+145	+107	24	0	+122	+90
				25	0	+131	+112
				26	0	+109	+64
				27	0	+147	+117
				28	0	+100	+54
				32	0	+215	+174
				33	0	+124	+123
				34	0	+98	+75
				35	0	+169	+91
				36	0	+128	+100
				37	0	+105	+66
				38	0	+138	+138
				Average expansion		+119	+96

TABLE 5

EXPOSED SPECIMENS

Gauge No.	5/10/66 Ten Min After Casting*	10/10/66 In Outside Exposure Hut at RRL
1	0	-202
2	0	-271
3	0	-264
4	0	-228
5	0	-233
6	0	-232
7	0	-205
8	0	-295

Discussion—The results indicate an overall expansion of the concrete in the structure in the first week as a result of hydration and cooling. The briquetted gauges generally indicate greater expansion than the unbriquetted ones; the average value for 13 briquetted gauges being 145×10^{-6} in./in. This may be the effect of the briquetted concrete being rewetted when the concrete for the structure is placed, or alternatively an effect associated with the temperature rise on hydration. It is probable, however, that when the initial readings are taken after the peak temperature of hydration has occurred, the strain values are the same as for unbriquetted gauges, as was observed for gauges of different types.

The average value of expansion recorded in one week from casting is greater than recorded in any of the other investigations. This appears to have arisen from the low coefficient of expansion of the limestone aggregate; e.g., for an ambient temperature of 20 C, a peak hydration temperature approximately 50 C, and a coefficient of expansion for limestone concrete of 7×10^{-6} per deg C (6, 11),

$$\text{strain change in wire on cooling} = 30 \times 12 \times 10^{-6} = 360 \times 10^{-6} \text{ in./in.}$$

$$\text{strain change in concrete on cooling} = 30 \times 7 \times 10^{-6} = 210 \times 10^{-6} \text{ in./in.}$$

As the gauge would be constrained to move with the concrete, an apparent expansion of 150×10^{-6} in./in. would be recorded on cooling, which would account for the high values of recorded expansion. This implies that on cooling a self-balancing set of forces is set up in the structure, the steel secondary reinforcement being in tension while the concrete is in compression, which would be beneficial in preventing possible early cracking. No cracks were, in fact, observed in the precast units. The average stress in the steel reinforcement after one week is evidently 119×10^{-6}, $\times 30 \times 10^{+6}$, i.e., about 3,500 psi, on the assumptions that all the initial expansion is transferred to the steel as indicated in the River Aire Bridge experiment, and the coefficients of expansion of the reinforcement and the wire of the gauge are the same, which is approximately true.

The results from the companion specimens show that normal shrinkage occurred; the average value being 241×10^{-6} in./in. in five months. This illustrates that the movement of a structure on the full-scale may be very different from that found in small specimens, and that care is needed in correlating results. A useful summary of coefficients of expansion for concretes made with various types of aggregate, due to Browne (11), is given in Table 6.

TABLE 6

VARIATION OF AGGREGATE AND NORMAL CONCRETE THERMAL EXPANSION WITH GEOLOGICAL ROCK GROUP*

Rock Group	Typical Silica Content (% by wt)	Thermal Expansion Coefficient of Aggregate (microstrain/deg F)				No. of Rock Specimens Tested	Thermal Coefficient of Expansion of Concrete (microstrain/deg F)	
		Minimum	Maximum	Maximum Variation	Mean		Minimum Recorded	Maximum Recorded
Chert	94	4.1 (7.4)	7.2 (13.0)	3.1 (5.6)	6.7 (11.8)	50	6.3 (11.4)	6.8 (12.2)
Quartzite	94	3.9 (7.0)	7.3 (13.2)	3.4 (6.2)	5.7 (10.3)	28	6.5 (11.7)	8.1 (14.6)
Quartz	94						5.0 (9.0)	7.3 (13.2)
Sandstone	84	2.3 (4.3)	6.7 (12.1)	4.3 (7.8)	5.2 (9.3)	43	5.1 (9.2)	7.4 (13.3)
Marble	Negligible	-1.2 (2.2)	8.9 (16.0)	10.1 (18.2)	4.6 (8.3)	35	2.3 (4.1)	4.1 (7.4)
Siliceous limestone	45	2.0 (3.6)	5.4 (9.7)	3.5 (6.3)	4.6 (8.3)	6	4.5 (8.1)	6.1 (11.0)
Granite	66	1.0 (1.8)	6.6 (11.9)	5.6 (10.1)	3.8 (6.8)	79	4.5 (8.1)	5.7 (10.3)
Dolerite	50	2.5 (4.5)	4.7 (8.5)	2.2 (4.0)	3.8 (6.8)	4		
Basalt	51	2.2 (4.0)	5.4 (9.7)	3.2 (5.7)	3.6 (6.4)	18	4.4 (7.9)	5.8 (10.4)
Limestone	Negligible	-1 (-1.8)	6.5 (11.7)	7.5 (13.5)	3.0 (5.5)	125	2.4 (4.3)	5.7 (10.3)
Gravel	5-95						5.0 (9.0)	7.6 (13.7)

*After Browne (11), based on survey of references.

NOTE: Figures in parentheses are thermal expansion coefficients in microstrain/deg C.

CONCLUSIONS

In general, the use of vibrating-wire gauges indicates expansion in concrete during setting up to the time of the peak hydration temperature: the maximum movement recorded was 170×10^{-6} in./in. when peak hydration temperatures were up to 30 C above ambient. An exception arose for a mix made with rapid-hardening portland cement where contractions up to 80×10^{-6} in./in. occurred.

Expansion has been recorded in quite small concrete specimens where there was very little rise in temperature during hydration. This suggests that the expansion arises from the change in state rather than from the temperature rise.

The amount of the expansion recorded depends on the stiffness of the barrel of the vibrating-wire gauge. In one experiment gauges manufactured with plastic tubes having a comparatively low stiffness showed almost double the movement recorded by steel- and brass-barreled gauges. The amount of movement was also shown to be greater near the top of the mold.

Readings taken on a simulated deck section, 12 in. thick, of the River Aire Bridge, using gauges attached to reinforcement and also a special tubular reinforcement gauge, suggest that where expansion occurs the reinforcement is also strained. For the deck section considered, the mean strain was 50×10^{-6} in./in. for which the equivalent tensile stress is 1,500 psi. Gauge readings taken on site confirmed the general pattern of expansion.

The shrinkage readings recorded from a zero taken at the time of peak hydration temperature (i.e., from the time when setting is assumed to be complete) using both types of RRL gauges and the BRS gauge show that the measured shrinkage is the same for all three gauge types; i.e., the movement of the concrete predominates once it has set.

Where the coefficient of expansion of the concrete is roughly the same as that of the steel wire of the gauge, i.e., 12×10^{-6} per deg C, which is true for gravel and quartzite aggregate concretes, the strain change in the gauge from the time of peak hydration temperature is a measure of the shrinkage from the condition of maximum volume; this being the shrinkage arising from moisture loss as opposed to contraction caused by temperature drop. Where the coefficients of expansion of the wire and concrete are not the same, a correction would need to be applied to allow for the temperature drop. Alternatively, if shrinkage readings are commenced when the concrete has cooled to ambient temperature then this difficulty is overcome. This is probably the most convenient zero from which to commence creep shrinkage measurements, but when prestress is applied at 1 or 2 days, an earlier zero must be taken. In the simulated deck experiment the value of shrinkage from the peak temperature was about 100×10^{-6} in./in. in two years, and very little of this occurred in the first months.

The contraction movement arising from temperature drop is far greater than that arising from shrinkage in the first few weeks after casting. For bridge decks, temperature drops of up to 45 C have been observed. The associated contraction would be about 500×10^{-6} in./in. in a gravel aggregate concrete. In addition, the more exposed parts of a bridge deck reach a lower peak temperature than thicker parts of the webs; differences of peak temperature of up to 30 C have been recorded. This gives rise to differential contractions on cooling with the possibility of early cracking.

When the strain change from the time of peak temperature is tensile, this indicates the presence of tensile stress due to differential cooling. In one investigation cracking was promoted at an early age when the maximum value of tensile strain reached 70×10^{-6} in./in. for a temperature difference of only 8 C. It is clear that temperature differences of this order are common during the casting of structural members.

In an investigation into the characteristics of an overhead road structure using limestone concrete, it has been demonstrated that, because of a value of low coefficient of expansion, cooling after hydration promotes tension in the secondary steel and compression in the concrete, the stress in the steel being approximately 3,500 psi.

The tests show that the movements of structures on the full-scale may be very different from the movements in control specimens and that care is needed in correlating results.

ACKNOWLEDGMENTS

The author wishes to express his thanks to the following staff of the Bridges Section, Road Research Laboratory, who assisted at various times in the investigations described in this report: M. W. R. Capps, M. Emerson, G. R. Bunn, P. Baxter, A. McKay, and J. Danby.

The author also wishes gratefully to acknowledge the assistance given to him by the Resident Engineer and staff of the West Riding of Yorkshire in obtaining the results from the River Aire Bridge; also by the staff of G. Maunsell and Partners for the Mancunian Way and by Concrete (Southern) Ltd., manufacturers of precast products.

This paper is published by permission of the Director of Road Research, British Crown Copyright, and reproduced by permission of the Controller of Her Britannic Majesty's Stationery Office.

REFERENCES

1. Some Applications of Vibrating-Wire Strain Gauges on Structures in the United Kingdom. Deakin Instrumentation Ltd., Data Sheet No. SG5/66, Walton-on-Thames, 1966.
2. Maihak, A. G. Remote Control Measurement for Concrete, Earth and Steel Structures. Pamphlet No. 1500E, Hamburg, 1961.
3. Potocki, F. P. Vibrating-Wire Strain Gauge for Long-Term Internal Measurement in Concrete. The Engineer, Vol. 206, No. 5369, pp. 964-967, 1958.
4. Browne, R. D., and McCurrich, L. H. The Measurement of Strain in Concrete Pressure Vessels. Conf. on Prestressed Concrete Pressure Vessels, Proc. Inst. Civil Eng. (London), March 1967.
5. Morice, P. B., and Base, G. D. The Design and Use of a Demountable Mechanical Strain Gauge for Concrete Structures. Cement and Concrete Association, C & CA Reprint No. 6, London, 1953.
6. Bonnell, D. G. R., and Harper, F. C. The Thermal Expansion of Concrete. National Building Studies, Tech. Paper No. 7, (HM Stationery Office, London, 1951).
7. Capps, M. W. R. Temperature Movements in the Medway Bridge—Interim Report. Road Research Laboratory, Laboratory Note No. LN/914/MWRC, Harmondsworth, 1965 (unpublished).
8. Emerson, M. Temperature Movements in the Hammersmith Flyover. Ministry of Transport, RRL Tech. Note No. 33, Crowthorne, Berkshire, 1966 (unpublished).
9. Corson, R. H. A New Gauge for the Measurement of Internal Strains in Concrete. Concrete and Constructional Eng., Dec. 1965.
10. Kier, M., and Hansen, F. Medway Bridge: Construction. Proc. Inst. Civil Eng. (London), Vol. 29, Paper No. 6812, Sept. 1964.
11. Browne, R. D. Properties of Concrete in Reactor Vessels. Conf. on Prestressed Concrete Pressure Vessels, Proc. Inst. Civil Eng. (London), March 1967.
12. L'Hermite, R. G., and McMillan, M. Further Results on Shrinkage and Creep Tests. Proc. Internat. Conf. on Structure of Concrete, London, 1965.
13. Tyler, R. G. Creep and Shrinkage in Prestressed Concrete at a Section of the Medway Bridge. Road Research Laboratory, Laboratory Note No. LN/594/RGT, Harmondsworth, 1964 (unpublished).
14. Kerensky, O. A., and Little, G. Medway Bridge Design. Proc. Inst. Civil Eng. (London), Vol. 29, Paper No. 6799, Sept. 1964.

Determination of the Consistency of Concrete By the Compacting Ratio Method

KURT WALZ, Forschungsinstitut der Zementindustrie, Düsseldorf, West Germany

The bulk density of a loosely charged concrete is dependent on its consistency. The relation of the volume of a loosely charged batch of concrete to the solid volume of this batch (for example after complete compaction) represents as "compacting ratio" a simple measure of the consistency.

For this procedure only a prismatic container and any tool for compaction (vibrator or tamper) are necessary. By this method the consistency of concrete with any maximum size of aggregate can be measured in the range from pulpy to stiff, and the compacting ratio extends from about 1.05 to about 1.50.

•THE determination of the consistency of concrete on construction sites requires a simple and sturdy device. Such an apparatus should reveal even slight changes in consistency and should be applicable to a large variety of concrete mixtures within wide limits of consistency. Since the existing methods for measuring consistency do not satisfy completely all these requirements, a new method has been developed, which is the subject of this paper. The procedure is based on the assumption that the denseness of a sample of uncompacted fresh concrete is controlled by its consistency. The acceptance of this method as a new German standard is under consideration.

The volume of a loosely charged batch of concrete, defined by the solid volume of cement and aggregate, is known to increase for concrete of stiffer consistency. A value for the consistency of the concrete will therefore be obtained by filling a definite prismatic container in always the same way with bulked (loose) concrete and by relating the volume of this loosely charged concrete to its solid volume determined by calculation, using the bulk specific gravity of the ingredients, or simpler by complete compaction (1, 2).

By always taking the same prismatic container, the volume of the bulked concrete and that of the completely compacted concrete is proportional to the height of the respective filling. Therefore, it is sufficient to relate only the height of the bulked filling, which is constant, to the height of the completely compacted filling. For concrete with aggregates up to 1½ in. maximum size, a sheet-steel container 16 in. high with an 8-in.-square cross section is used in practice. Also a cylindrical container of corresponding size will be suitable.

DETERMINATION OF THE COMPACTING RATIO

This procedure is shown in Figure 1. The following special devices are necessary (Fig. 2): a sheet-steel container 16 in. high with an 8-in.-square cross section, trapezoid-shaped trowel 4 by 6.5 in., straightedge, and foot rule. For testing the concrete, a quantity of at least 1 cu ft should be taken from different places of the mix and thoroughly mixed by hand. (By this method segregation will be avoided and parties that have already been precompacted during transport of the concrete to the testing device

Paper sponsored by Committee on Mechanical Properties of Concrete and presented at the 47th Annual Meeting.

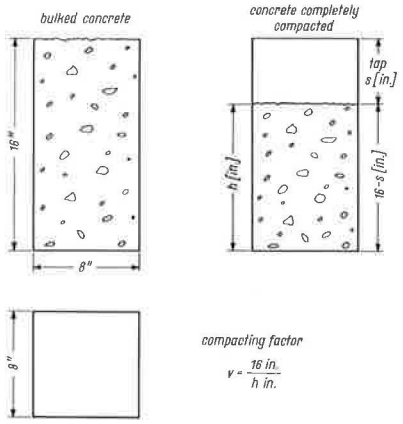

Figure 1. Determination of compacting ratio v by means of a container 16 in. high with an 8-in.-square cross section.

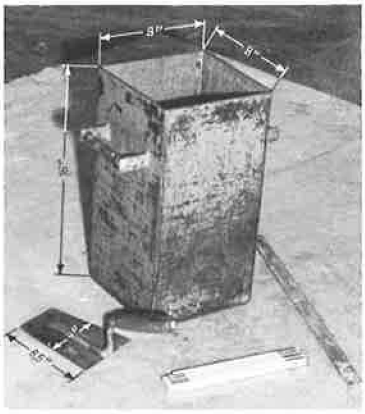

Figure 2. Equipment for determination of compacting ratio: steel-sheet container 16 by 8 by 8 in.; trowel 4 by 6.5 in.; straightedge; and foot rule.

will be loosened again.) As shown in Figure 3, the concrete is slowly dumped from a longitudinal edge of the fully loaded trowel into the container over its border. This is continued by turns over each of the four borders until the 16-in.-high container is slightly overfilled; then it is smoothly struck off (height of the filling 16 in.). Afterwards the dumped concrete is continuously compacted in some way, at best by an internal vibrator (Fig. 4), until there is no further sinking. After having leveled the surface, the height h (average) of the completely compacted filling (h = 16 in.) is

Figure 3. Filling of the container by slowly dumping concrete from trowel over borders of container.

Figure 4. Complete compaction of loosely charged concrete by a vibrator centrally inserted into the container (also possible by intensive tamping).

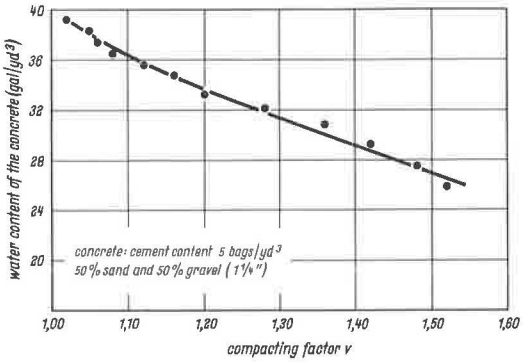

Figure 5. Compacting ratio v of a concrete with varying water content (28 to 40 gal/cu yd).

determined by measuring at four or more points. The consistency is measured by the compacting ratio

$$v = \frac{16}{h}$$

EXPERIMENTAL INVESTIGATIONS

Influence of the Water Content

When plotting water content against the compacting ratio of concrete with the same aggregate and cement content (Fig. 5), a strong dependence is evident. In plastic as well as in the stiff range, a relatively slight variation in the water content of the concrete resulted in a remarkable alteration of the compacting ratio. Figure 6 shows the results of concrete with the same aggregate; however, with different cement contents ($4\frac{1}{2}$ to 6 bags/cu yd).

Reproducibility

In order to evaluate the standard deviation of the test procedure caused by various persons, the compacting factor of a stiff and a plastic concrete was measured in turns by eight partly unskilled laboratory workers. The cement content was about 5 bags/cu yd; the aggregate consisted of 50 percent sand and 50 percent gravel ($1\frac{1}{4}$ in.).

The results for the stiff concrete were in succession

$$v = (1.42 + 1.43 + 1.42 + 1.44 + 1.45 + 1.45 + 1.45 + 1.47) : 8 = 1.44$$

The standard deviation was less than 0.02; it was, however, calculated from eight values only and included also the alteration by increasing stiffening of the concrete batch during the testing time of about $1\frac{1}{2}$ hours. The results for the plastic concrete were as follows:

$$v = (1.19 + 1.21 + 1.20 + 1.25 + 1.22 + 1.22 + 1.22 + 1.25 + 1.24) : 8 = 1.22$$

with a standard deviation of less than 0.02.

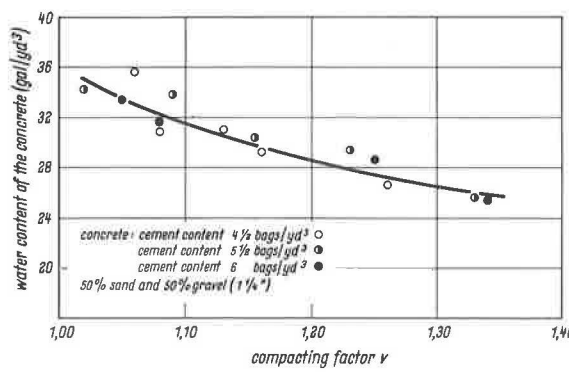

Figure 6. Compacting ratio of concrete with varying water content and cement content.

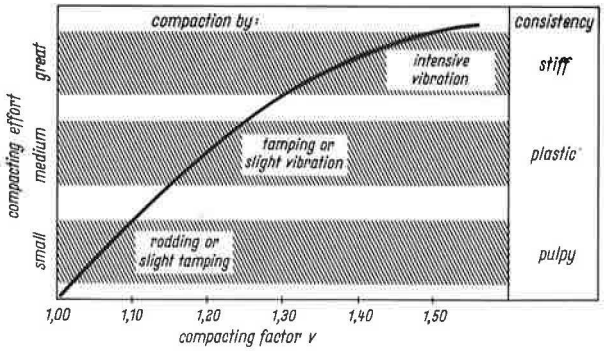

Figure 7. Compacting ratio (consistency) and compacting effort for concrete with aggregate 0-1¼ in.

Compacting Ratio and Compacting Effort

Figure 7 shows the relation between compacting effort and compacting ratio. For the compaction of concrete with a compacting ratio of 1.40, for example, on the building site, intensive vibration is necessary.

SUMMARY

The consistency in the range from stiff to pulpy concrete can reliably be measured by the compacting ratio v. It reacts already on small variations in the water content of a concrete mix. The procedure is easy, only simple and sturdy devices are needed. The exactitude of indication of this method (standard deviation) is quite satisfactory, if the test instructions are observed. The procedure can also be applied to measure the consistency of mass concrete with very coarse aggregates when a container of corresponding size is used.

REFERENCES

1. Walz, K. Workability and Mechanical Properties of Fresh Concrete (in German). Deutscher Ausschuss für Stahlebeton, No. 91, pp. 37-38, 1938.
2. Walz, K. Vibrated Concrete (in German). First Edition, Wilhelm Ernst and Sohn, Berlin, 1944, 17 pp.

Analysis of The Influence of Water Content on Consistency

SANDOR POPOVICS, Auburn University

This paper presents an analysis of the change in consistency that is caused solely by a change in the water content. A numerical method—the so-called K-procedure—is discussed in detail. It is a simple tool for the calculation of a needed adjustment in the water content of cement paste, mortar, or concrete. The K-procedure is based on the assumption of independence. Predicting formulas are offered for various methods of measuring consistency, and a mechanism is presented for the role of water in fresh mixtures. This mechanism explains why an increase in the water content causes a greater than linear increase in the mobility of a fresh mixture. Numerical examples illustrate the use of the K-procedure. To assist with practical application, tabulated data and nomograms are provided for the K-factors of several standard test methods.

•THE rheology of liquid-solid suspensions in terms of concentration is the target of numerous theoretical and empirical investigations that, in turn, result in a variety of formulas (1, 2, 3). However, there are difficulties with the application of these results for a fresh concrete, caused primarily by the heterogeneity of the concrete mixtures. This is highly unfortunate because it is almost impossible to overestimate the technical importance of the flow properties of a fresh concrete. Thus, the current absence of an adequate theory forces the concrete technician to be content with empirical or semi-empirical approaches concerning these properties and to deal with such ill-defined concepts as consistency and workability (4).

This paper presents a technical analysis of the change in consistency caused solely by the change in water content. Such an analysis requires the reexamination of previously published hypotheses and experimental data concerning the role of water in the rheological behavior of fresh paste or concrete. In some instances this leads to new findings, such as the estimate of the amount of the non-lubricating water, in others to inferences not intended by the original author. It is anticipated that this unified presentation can contribute to a better understanding of the complex problem of consistency and workability, and can aid in future research.

Mathematical derivations and most of the standard consistency measurements for experimental justification of the formulas are omitted for the sake of brevity. Interested readers can find these details in numerous references noted in the text.

ASSUMPTION OF INDEPENDENCE AND THE K-PROCEDURE

The change in consistency of fresh mixtures—such as cement pastes, mortars, concretes, and soil-water mixtures—seems to follow a complicated pattern even when this change is due only to a variation of the water content. It is true that an increase in the water content results in a softening of the mixtures. However, an increase of, say, one gallon in the water content of a batch, with the composition and quantity otherwise

Paper sponsored by Committee on Mechanical Properties of Concrete and presented at the 47th Annual Meeting.

unchanged, will cause changes of differing magnitudes, depending upon the initial water content, consistency, and the method of measuring the consistency. Fortunately, this situation is greatly simplified with the adoption of the following assumption of independence (5, 6, 7, 8): The amount of change in consistency which is due solely to the (relative) change in water content of the mixtures is independent of the composition of the mixture.

To illustrate the assumption of independence, assume that the slump of a concrete should be increased from a value of 2 in. to 3.5 in. by adding water to the mixture; also assume that this requires a 5.5 percent increase in water content for the given concrete composition. According to the assumption of independence, the 5.5 percent increase in water content will result in an increase of slump from 2 to 3.5 in. for every concrete composition. A less precise form of the assumption of independence is the rule of thumb (used by concrete technicians in the 1920's and 1930's) that a stiff consistency of any concrete can be made plastic by increasing the water content 15 percent. Experimental results justify the use of the assumption of independence within wide limits.

The numerical method which is based on the assumption of independence is called the "K-procedure" because the fundamental equation of this method is

$$w_2 = Kw_1 \tag{1}$$

where

w_1 and w_2 = water content of a fresh mixture for the initial consistency and the changed (predicted or desired) consistency respectively; and
K = thinning factor which is independent of the composition of mixture.

It follows from Eq. 1 that, for instance, $K = 1.10$ means a 10 percent increase in the water content of the mixture, and $K = 0.90$ means a 10 percent decrease.

It was shown mathematically that if indeed the assumption of independence is true, then the consistency measure, for instance slump, as well as the K factor in Eq. 1, are necessarily power functions of the water content as follows (5, 6, 7, 8):

$$y = c_1 w^i \tag{2}$$

and

$$K = (y_2/y_1)^{1/i} \tag{3}$$

where

y = specified consistency measure (e.g., slump),
w = water content of the fresh mixture,
c_1 = parameter which depends on the composition of the mixture and method of measuring consistency,
i = test method constant which is independent of the composition of the mixture but depends on the method of measuring consistency,
K = thinning factor, and
y_1 and y_2 = consistency measure of the mixture for the initial consistency and for the changed (predicted or desired) consistency respectively.

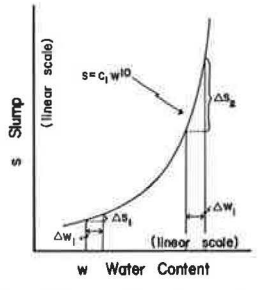

Figure 1. Change in slump due to the change in water content.

The K-procedure, therefore, is a method where the change in consistency, which is due solely to the change in water content, is approached by a power function defined by Eqs. 2 and 3. That is, the assumption of independence is a qualitative form, and Eqs. 1, 2, and 3 are quantitative forms of the same phenomenon concerning consistency as a function of water content.

The graphical representation of the relationship for consistency vs water content, such as Eq. 2, is

TABLE 1

VALUES OF "i" AND THE CONSISTENCY LIMITS OF THE K-PROCEDURE*

Test	Designation	i	Consistency Limits
Test for normal consistency of hydraulic cement (Vicat test)	ASTM C 187-58 BS 12 DIN 1164	15	6 - 30 mm
Flow table for use in tests of hydraulic cement	ASTM C 230-57 T DIN 1164	3	55 - 130%
Test for slump of portland cement concrete	ASTM C 143-58 BS 1881	10	2 - 6 in.
Test of penetration for portland cement concrete	DIN 1048	6	2 - 20 cm
Modified remolding test for portland cement concrete	ONORM B 2303	-9	80 - 5 kg/cm^2
Compacting factor test for portland cement concrete	BS 1881	0.01c - 1.7	0.75 - 0.95
Test for liquid limit of soils	ASTM D 423-61 T	-8.3	20 - 30

*From Ref. (8).

called the "consistency curve" (Fig. 1). The rate and the specific rate of consistency change caused solely by the change in water content are defined as dy/dw and (dy/dw)/y respectively. It can be shown that the absolute value of the "i" power is approximately equal to this specific rate of consistency change for the practical range of the w values. Therefore, this value can be used for the characterization of any method of measuring consistency, as long as the value of "i" can be considered independent of the composition of concrete.

The "i" values for several methods of measuring consistency have been determined experimentally (5, 6, 9) and are given in Table 1. The same table also contains the empirical consistency limits for the methods within which the K-procedure is valid. The other limits of validity for the K-procedure, in general, are the confines of adequate workability, such as cement content higher than 400 lb/cu yd, not too coarse aggregate grading, etc.

Example 1

What change in the water content of a concrete will increase the slump from 2 to 5 in. provided that the composition of the concrete remains otherwise unchanged?

Solution: Since the "i" test method constant for the standard slump test is equal to 10 (Table 1), therefore Eq. 3 provides the following K factor:

$$K = (\tfrac{5}{2})^{0.1} = 1.10$$

Hence, if the water content of the 2-in. slump concrete is w_1, then the w_2 water content that will produce a 5-in. slump is

$$w_2 = 1.10\, w_1$$

APPLICATION OF THE K-PROCEDURE

Analyses of a variety of experimental data demonstrated that the changes in consistency, which are due solely to the changes in water content, can be approximated by power functions of Eqs. 2 and 3 for many methods of measuring consistency (5, 6, 7, 8, 9, 10, 11, 12, 13, 14). A noteworthy exception is the standard British compacting factor test, BS 1881, for which a modification of Eq. 3 is necessary (9). A recent paper by Newman (15) also supports this modified thinning factor for the CF test.

Various forms can be obtained by simple algebraic manipulations for the previously mentioned equations of the K-procedure. One such form is

$$y_2 = y_1 (w_2/w_1)^i \qquad (4)$$

where the symbols are the same as in Eqs. 1 and 3.

Other forms are

$$y_2 = y_1\left(w_{rel}\right)^i \tag{5}$$

$$y_{rel} = \left(w_{rel}\right)^i \tag{6}$$

$$Y_{rel} = \left(1 + W_{rel}\right)^i - 1 \tag{7}$$

where

$w_{rel} = w_2/w_1 = K$ = relative water content,
$y_{rel} = y_2/y_1$ = relative consistency measure,
$W_{rel} = (w_2 - w_1)/w_1$ = relative change in water content, and
$Y_{rel} = (y_2 - y_1)/y_1$ = relative change in consistency measure (16).

The use of these equations is illustrated in Example 2.

For practical application, the numerical values of the various K factors can be arranged either in tabulated form or in nomograms. For instance, Table 2 gives the numerical values of the K factor for the standard slump test (ASTM C 143-58 or BS 1881:1952 (17)). Their use is also illustrated by Example 1. Nomograms are shown in Figures 2 and 3 where the K-procedure is presented for the standard Vicat penetration test (ASTM C 187-58 or BS 12:1958 or DIN 1164), and for the standard flow test for cement mortar (ASTM C 230-57T or DIN 1164), respectively. Further tables and nomographs for the K-procedure can be found in the literature (5, 6, 7, 8, 9, 18, 19, 20).

Example 2

Assume that the amount of mixing water of a concrete batch that gives y_1 = 2-in. slump with w_1 = 10 gallons of water is increased by 1 gallon, i.e., w_2 = 11 gallons. What increase in slump can be expected from the new batch provided the composition of the batch remains otherwise unchanged? For the standard slump test, i = 10.

Solution: By using Eq. 5

$$w_{rel} = {}^{11}/_{10} = 1.10$$

$$y_2 = 2(1.10)^{10} = 5 \text{ in.}$$

By using Eq. 6

$$y_{rel} = (1.10)^{10} = 2.50$$

that is, y_2 will be 250 percent of the initial 2-in. slump.

By using Eq. 7

$$W_{rel} = {}^{1}/_{10} = 0.1$$

$$Y_{rel} = (1.10)^{10} - 1 = 1.50$$

that is, a 10 percent increase in the water content will cause a 150 percent increase in the initial slump of 2 in.

TABLE 2

THINNING FACTOR K FOR VARIOUS SLUMPS*
(Calculated by Eq. 3 with i = 10)

From y_1	To y_2								
	1	1.5	2	2.5	3	4	5	6	7
1	1.00	1.04	1.07	1.10	1.12	1.15	1.18	1.20	1.22
1.5	0.96	1.00	1.03	1.05	1.07	1.10	1.13	1.15	1.17
2	0.93	0.97	1.00	1.02	1.04	1.07	1.10	1.12	1.13
2.5	0.91	0.95	0.98	1.00	1.02	1.05	1.07	1.09	1.11
3	0.89	0.93	0.96	0.98	1.00	1.03	1.05	1.07	1.09
4	0.87	0.91	0.93	0.95	0.97	1.00	1.02	1.04	1.06
5	0.85	0.89	0.91	0.93	0.95	0.98	1.00	1.02	1.04
6	0.83	0.87	0.89	0.91	0.93	0.96	0.98	1.00	1.02
7	0.82	0.86	0.88	0.90	0.92	0.94	0.96	0.98	1.00

y_1 = initial slump, in.
y_2 = changed or expected slump, in.

*From Ref. (17).

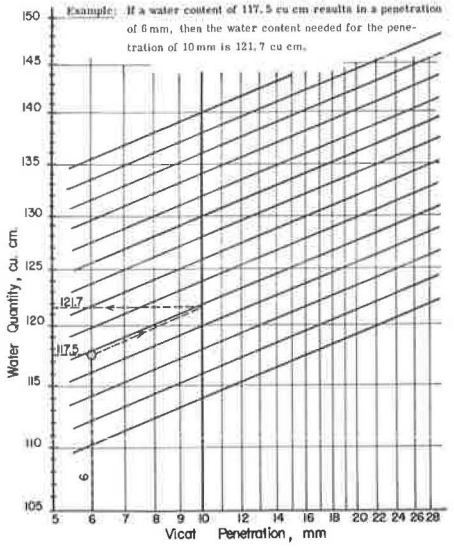

Figure 2. Estimation of water content of cement paste (with 500 g cement) needed for a specified penetration (20).

MECHANISM OF CHANGE IN CONSISTENCY

The mechanism of the change in consistency of a concrete can be approached through the consistency change of the cement paste. The related pioneering research was done by Powers (21, 22).

The plasticity of a cement paste can be attributed to a combination of attractive forces between particles and the lubricating action of the water between particles. The first few molecular layers of water absorbed immediately on the surface of cement particles consist of oriented molecules that are kept more or less immobile (23, 24). With an addition to the liquid content, the absorbed water layers become thick enough so that the outermost ones are not composed of well-oriented water molecules; thus, they may have a certain mobility while still lacking noticeable lubricating properties. This is so because in addition to the oriented water absorbed in the surface, a relatively large portion of water is believed to be enclosed in pores and surface "pockets" of the particles in a liquid or semi-liquid condition in such a manner that it has little lubricating effect. The lubricating action (hence, the plastic state) would develop only after increasing the water content of the paste beyond a w_o limit. The w_o limit can be called the non-lubricating water content, and it characterizes the maximum amount of water for a given material and method of testing with which the paste does not show a tendency to flow under the unsustained application of a force. It is obvious from this mechanism that the previously presented equations are strictly valid only for that fraction of the total water content which has the lubricating effect in the mixture. The structural meaning of w_o is not clear and its determination is also uncertain. Fortunately, the analysis of experimental results demonstrates that the simplification of using the total water content in mortars and concretes of usual composition does not impair the reliability of the K-procedure significantly.

When the water content is great enough to have a lubrication effect but is still low enough that the air voids exceed the water-filled space, the cohesion of the paste depends mostly on the intensity of the capillary tension and on the fraction of cross-sectional area occupied by the water (25). This cohesion can be expressed numerically in terms of particle size, porosity of packing, water content, etc., by using certain simplifying assumptions (26).

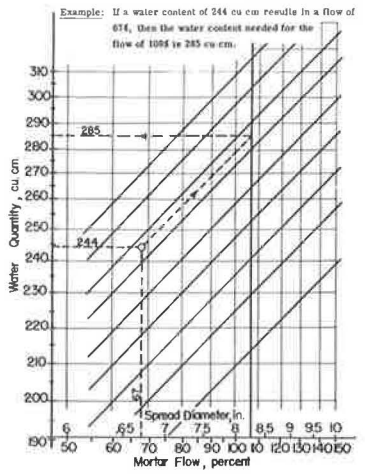

Figure 3. Estimation of water content of standard mortar (with 500 g cement) needed for a specified flow (20).

When the water content is progressively increased, the cohesion first increases, then rapidly decreases (27) because the capillary tension also decreases rapidly and the air spaces become smaller. Finally, a point is reached where the capillary tension has disappeared because the water has isolated the open air spaces into air bubbles by partially filling these spaces. This particular state can be demonstrated by electrical measurements because the electrical resistance of a cement paste as a function of water content shows a sudden drop at this point (28). Powers calls this water content "basic water content," and the related consistency is "basic consistency" (21). The remaining cohesive force in a paste of basic consistency is a result solely of interparticle attraction between cement particles.

Therefore, this consistency is the stiffest to allow true plastic deformation and permit compaction by a low-energy procedure. The basic consistency for a cement paste is about the same as the standard normal consistency. For concretes, it corresponds to a slump of 1 to 2 in.

The increase of water content beyond the basic water content causes the consistency to become softer rapidly because it results in a greater dispersion of cement particles, i. e., a reduction in the cohesive force, a greater freedom for the individual particles, more lubrication, and hence, a greater than linear increase in the mobility of the paste.

This mechanism is only slightly changed when a surface-active agent is used as a water-reducing admixture in the paste. Such molecules tend to become concentrated and form a film at the interface between cement and water, and alter the physiochemical forces acting at this interface (29). The mobility of such a plastified paste becomes greater partly because of a reduction in the interparticle forces and partly because of a reduction in w_o (30).

When cement paste and aggregates are combined into mortar or concrete, the paste has a role similar to that which the water had in the paste. That is, the cement paste provides cohesion for the total mixture and also acts as a lubricant between aggregate particles. It is important to recognize, however, that the consistency of a concrete becomes stiffer than that of the paste alone because of the interference of aggregate particles. The larger the amount of aggregate in the mixture, the stiffer the consistency appears. Therefore, three possibilities are available to soften the consistency of a concrete without changing the quality of the components: first, the amount of cement paste can be increased by keeping the water-cement ratio, thus the consistency of the paste, constant; second, the consistency of the paste can be softened by using higher water-cement ratio but without increasing the paste volume; and third, these two methods can be combined. In all three cases the water content of the total mixture increases, and this can be considered as a primary reason for the softening of concrete consistency. It is necessary to note, however, that apart from other harmful consequences, the thinning of cement paste beyond a certain limit does not soften the consistency of concrete because a fluid-like paste is unable to disperse the aggregate particles (31). A more refined discussion of the interparticle forces in fresh concrete is given in recent papers by Powers (32, 33).

An additional factor to be considered is the effect of hydration reactions on the consistency of the cement paste, especially because these reactions begin almost immediately when the cement contracts the water (34, 35). Experience shows that in the case of standard portland cements, the developing hydration products do not influence noticeably the plasticity of the paste within reasonable time limits. Thus, it may be concluded that the presented mechanism of the change in consistency explains why a reasonable increase in the water content causes a greater than linear increase in the mobility of the fresh mixture.

JUSTIFICATION OF THE K-PROCEDURE IN PRINCIPLE

Although the presented mechanism of change in consistency provides only a qualitative basis for the K-procedure, certain other considerations support this procedure in principle also. Such a consideration is the recall of the experimental fact that the K-procedure is applicable to cement pastes (6, 8, 11).

Another significant consideration is that not only the results of consistency tests, which are set up more or less arbitrarily, can be approached well with a power function but also characteristics of the fresh mixture that are fundamental to the complex property of workability. The viscosity is one such characteristic. According to Figure 4, measurements by Komlos (36) demonstrate that the degree of viscosity of a cement mortar measured in a rotational viscometer is a power function of tenth degree of the water content with a good approximation (8, 9). A similar analysis of the measurements by Nessim and Wajda (37) obtained with a rotational viscometer also shows (Fig. 5) that both the total energy input and the plastic viscosity of a cement paste or mortar can be expressed approximately as a power function of fifth degree of the water content. It is also significant that according to Orr and Blocker (38) the relative

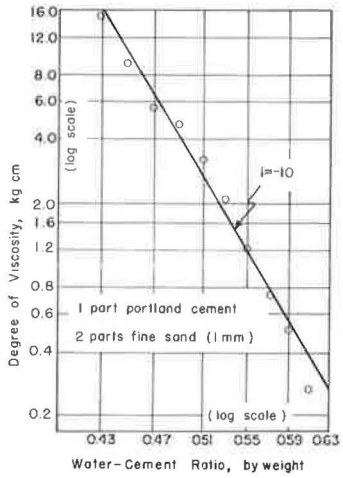

Figure 4. Viscosity of a cement mortar, measured with a rotational viscometer, as a function of water content (36).

viscosity of a wide range of suspensions of spheres increases as a power function with suspension concentration.

A different but important characteristic of the fresh concrete mixture is the minimum time of vibration needed for the complete compaction of the concrete. According to Figure 6, two test series by Plowman (39, 40) as well as a test series by Spindel (12) demonstrate again that these minimum times of vibration are also power functions of the water content with a good approximation (7, 8, 14). Thus, one may say with a little license that the K-procedure can express the change in workability of concrete as a function of the water content.

As has been mentioned before, the equations presented in this paper are valid strictly for that amount of water in the mixture which has a lubricating effect. Therefore, the correct form of Eq. 2 is

$$y - y_o = c_2 \left(w - w_o \right)^i \qquad (8$$

where

y_o = value characteristic of the consistency of water,
w = total water content of the mixture,
w_o = amount of non-lubricating water, and
c_2 = parameter which depends on the composition of mixture and method of measuring consistency.

The other symbols are identical with the symbols of Eq. 2. A graphical representation of Eq. 8 is shown in Figure 7 for a negative i.

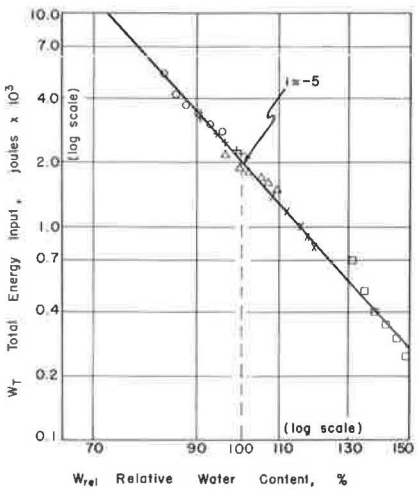

Figure 5. Viscosity of a cement paste, expressed as "total energy input" of a rotational viscometer at five different angular speeds, as a function of relative water content (37).

The value of w_o depends decisively on the specific surface of the solid particles in the mixture. This specific surface of mortars and concretes of usual compositions is relatively low; therefore, the use of the approximation of $w_o = 0$ is reasonable for these mixtures, along with the approximation of $y_o = 0$, as far as the K-procedure is concerned, provided that the c_1 parameter of Eq. 2 is chosen properly. The specific surface of a powder is much greater; thus, the value of w_o for pastes may be quite high. To illustrate this point, one can refer to a test series by Powers where he measures the consistencies of pastes made with six different powders and gradually changing water contents (22). He uses the "t" time for flow of paste under a pressure of one psi from a 100 cc pipette to characterize the consistency. His apparatus provides about 5 seconds time of flow for water and $i = -5$ for the test method constant. Thus, the t consistency of any of his pastes can be expressed by the following formulas as a function of the water content:

$$t - 5 = c_2 \left(w - w_o \right)^{-5} \qquad (9)$$

where w represents the percent water in the pastes by absolute volume.

Tables 3 gives the values of c_2 and w_o for the pastes. These values are determined by the slopes and intercepts of the fitted straight lines in the special system of coordinates of Figure 8. The figure demonstrates also that the goodness of fit between Eq. 9 and the experimental results is highly satisfactory. In addition, Eq. 9, with the factors of Table 3, represents curves that converge to the value of t = 5.1 seconds with a good approximation when the solid contents of the pastes approach zero. It should be noted that the values in Table 3 are valid only for the apparatus and test method used by Powers in his experiments. A more vigorous method of measuring consistency would leave a smaller amount of non-lubricating water around the solid particles in the pastes.

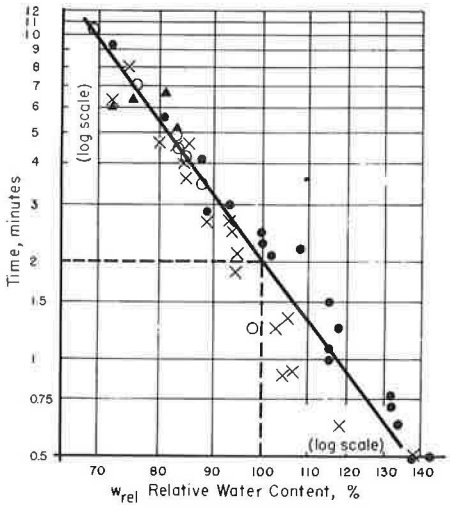

Figure 6. Relationship between time of vibration for full compaction and relative water content (39).

It is probably more than a coincidence that the analysis of bleeding results of portland cement pastes has led to the introduction of a "stagnant" water content for the initial rate of bleeding which is similar to the concept of w_o (41, 42). Steinour concludes from his pertinent experiments that this stagnant water content generally lies between 24 and 32 percent for the usual portland cements and the applied test method.

Finally, it should be mentioned that there have been numerous experiments concerned with the applicability of the approximation by power function to the consistency of soil-water mixtures (43). The conclusion of these tests is affirmative to such an extent that the procedure is standardized as a rapid or one-point method by ASTM for the determination of liquid limit of soils (ASTM D 423-61T). In addition, the assumption of independence is also suitable for properties of soil-water mixtures other than consistency. Data from the technical literature indicate that power functions may be applicable as a simple approach to penetration resistance, shearing strength, electrical resistivity, and moisture retention of soil-water mixtures as a function of water content (7).

OTHER TYPES OF THINNING FACTOR

In addition to the form of power function, several other types are also recommended for the thinning factor both in the concrete technology and in soil mechanics. The chronologically first thinning factors evaluated the consistency according to appearance (stiff, plastic, etc.), i.e., not numerically; therefore, at present they are of only historical interest. Such qualitative thinning factors are, for instance, the relative consistency recommended by Abrams (44), the relative water content by Talbot and Richart (45), and the water factor of Young (46).

Probably the first thinning factor for concrete, utilizing numerical consistency measures, had a logarithmic form which was set up empirically. For a certain fixed y_1 basic consistency and for a modified remolding test (ONORM B 2303), the following thinning factor was recommended (47):

$$K_{log} = (a - \log y_2)/b \qquad (10)$$

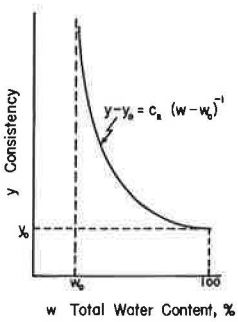

Figure 7. The non-lubricating water content w_o.

TABLE 3

PARAMETERS OF THE CONSISTENCY EQUATION FOR THE PASTES TESTED BY POWERS

Powder	c_2 (sec)	w_0 (%)
Portland cement	3.12×10^8	22.5
Pumicite	1.26×10^8	34.2
Hydraulic lime	0.925×10^8	39.2
Hydrated lime	1.50×10^7	55.8
Celite	1.27×10^5	80.3
Aquagel	4.47×10^3	92.2

NOTE: w_0 is the amount of non-lubricating water. Both c_2 and w_0 are dependent on the quality of particle surface, specific surface, and method of measuring consistency.

where

K_{log} = logarithmic thinning factor,
y_2 = consistency measure for the changed (predicted or desired) consistency measured by the specified method, and
a, b = test method constants which include the effect of the particle shape, as well.

A more general form of Eq. 10 is

$$K_{log} = 1 + \frac{1}{i_1}\left(\log \frac{y_2}{y_1}\right) \qquad (11)$$

where i_1 is the test method constant for this type of thinning factor. The other symbols are the same as those used in Eq. 3. For the standard slump test, the value of i_1 is approximately 4. 2.

It appears, at first, that the use of the K_{log} factor is incompatible with the assumption of independence because it is not a power function of the consistency measure. Further analysis reveals, however, that there is no serious contradiction. The logarithmic thinning factor is very close to the thinning factor of power function in several respects. For example, Eq. 11 can be written

$$K_{log} = 1 + \log\left(\frac{y_2}{y_1}\right)^{1/i_1} \qquad (12)$$

which is similar to the form of Eq. 3. A more fundamental relationship between the two types of thinning factor is: Eq. 10 or Eq. 11 represents the first approximation of the K of power function. This approximation is obtained by omitting the terms of second and higher degrees from the Taylor's series of Eq. 3 (7, 8).

It is easy to show that the consistency curves corresponding to the K_{log} factor are exponential functions that form a family of converging straight lines in a w vs log y semilogarithmic system of coordinates and the point of convergence is on the w = 0 axis. It has been demonstrated mathematically that such exponential functions will provide a family of parallel straight lines for the consistency curves in a log-log system with a very good approximation. Extent of approximation is shown elsewhere (7, 8).

With Eq. 11, various forms can be obtained for Eq. 1, similarly to Eqs. 4 through 7. One such form is

$$W_{rel} = \frac{1}{i_1} \log y_{rel} \qquad (13)$$

where the symbols are identical with the symbols of Eqs. 6 and 7. This equation indicates that K_{log}, along with the corresponding exponential consistency curve, has a physical interpretation which can be expressed as a slightly modified assumption of independence.

Arrhenius (48) is the first to apply an exponential form for the viscosity-vs-concentration relationship of diluted liquids. He arrives at this function empirically, by curve fitting. Similar exponential function is utilized for concrete consistency first by Austrian (47) and later by French investigators (49, 50, 51). Recently,

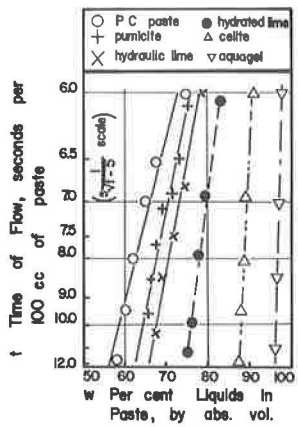

Figure 8. Relation of consistency of paste to composition. Measurements obtained by Powers (22) by timing flow under a pressure of 1 psi from a pipette.

Powers (33) presented a favorable appraisal for the foundation of this approach, i. e., of the K_{log}. This should not be surprising despite all the evidence presented for the approximation by power function. As indicated, the differences between the values calculated with the K and K_{log} procedures, respectively, are practically negligible; therefore, on this basis, no preference can be given to either method. There is, however, an additional consideration that favors the approximation by power function. So long as K is used as a multiplying factor (as in Eq. 1) and is assumed to be independent of the composition of the mixture, the power function is the logical choice because it was derived precisely from these two conditions. Consequently, at the present state of concrete technology, this method seems technically the most suitable for describing the change in consistency caused by the change in water content.

Two further forms for the thinning factor can be derived from Eq. 3 by an expansion into binomial series. This expansion is recommended by Mohan and Goel (52) for the simplification of the calculation of thinning factor. One of these forms is linear:

$$K_{lin} = 1 - 1/i + (1/i)\,(y_2/y_1) \tag{14}$$

where the symbols are the same as in Eq. 3. Eq. 14 is recommended mainly for methods where the consistency measure increases with an increase in water content, i. e., when $i > 0$. Because of its simplicity, however, it might be considered for use even when i is negative.

The second form is the hyperbolic, which is employed primarily for the cases when i is negative:

$$K_{hyp} = \frac{1}{1 + 1/i - (1/i)\,(y_2/y_1)} \tag{15}$$

where the symbols are the same as in Eq. 3. Further comparison of the various types of thinning factor can be found in the literature (7, 8).

CONCLUSIONS

The application of the assumption of independence and that of the K-procedure are justified within wide limits for many methods of measuring consistency and is recommended for use.

The same amount of added water causes less softening with a dry initial consistency than with a plastic. However, within wide limits, the same amount of relative change in the water content causes the same amount of relative change in the consistency measure regardless of the consistency and composition of the mixture. This rule is as fundamental to the consistency as the water-cement ratio vs strength relationship to the hardened concrete.

Among the various forms of the K-factor, the power function form (represented by Eq. 3) is recommended because of its identity with the assumption of independence. Tables or nomograms make the practical application easy.

REFERENCES

1. Rheology Theory and Applications (F. R. Eirich, editor), Vol. 3. Academic Press, New York and London, 1960.
2. Moavenzadeh, F., and Stander, R. R., Jr. On Flow of Asphalt. Highway Research Record 134, pp. 8-35, 1966.
3. Biggs, W. D. Theoretical Background. In Composite Materials (L. Holliday, editor), Elsevier Publishing Co., Amsterdam/London/New York, pp. 28-64, 1966.
4. Popovics, S. Workabilité et consistance (Workability and Consistency). Materials and Structures—Research and Testing, Vol. 1, No. 1, Paris, Jan.-Feb. 1968.
5. Popovics, S. Problems of Calculation of Concrete Mixtures. Acta Technica Academiae Scientiarum Hungaricae, Vol. 11, Nos. 1-2, Budapest, 1955.
6. Popovics, S. Relationship Between the Change of Water Content and the Consistency of Fresh Concrete. Mag. of Conc. Res., Vol. 14, No. 41, pp. 99-108, London, July 1962.

7. Popovics, S. Predictability of Certain Properties of Soil-Water Mixtures. Highway Research Record 63, pp. 10-21, 1964.
8. Popovics, S. Über den Einfluss des Wassergehalts auf die Konsistenz (Influence of Water Content on the Consistency). Betonstein-Zeitung, Vol. 32, No. 12, pp. 684-692, Dec. 1966.
9. Popovics, S. Some Aspects of Methods for Measuring Consistency. Mag. of Conc. Res., Vol. 17, No. 50, pp. 15-20, March 1965.
10. Duriez, M., and Arrambide, J. Nouveau traité de matériaux de construction (New Treatise of the Materials of Construction). Dunod, Paris, Vol. 1, pp. 1313-1315, 1961.
11. Popovics, S. Author's closure on discussion of Ref. 17. ACI Jour., Proc., Vol. 61, No. 9, pp. 1176-1181, Sept. 1964.
12. Spindel, J. E. Discussion of Ref. 6. Mag. of Conc. Res., Vol. 16, No. 47, pp. 114-115, June 1964.
13. Popovics, S. Discussion of "Proposed Standard Recommended Practice for Selecting Proportions for No-Slump Concrete" by Subcommittee 2, ACI Committee 211. ACI Jour., Proc., Vol. 62, pp. 1132-1135, Sept. 1965.
14. Popovics, S. Author's closure on discussion of Reference 9. Mag. of Conc. Res., Vol. 17, No. 53, pp. 218-219, Dec. 1965.
15. Newman, K. Properties of Concrete. Structural Concrete, Vol. 2, No. 11, pp. 451-483, Sept./Oct. 1964.
16. Popovics, S. Discussion of "Measurement of the Workability of Concrete" by U. T. Meyer. ACI Jour., Proc., Vol. 60, No. 3, March 1963.
17. Popovics, S. Tables for Concrete Mix Proportioning. ACI Jour., Proc., Vol. 61, No. 1, pp. 45-56, Jan. 1964.
18. Popovics, S. Consistency and Its Prediction. RILEM Bull. No. 31, pp. 235-252, Paris, June 1966.
19. Nasser, G. D. Some Notes on High Strength Steel, Pavement Scaling, and Slump Control. ACI Jour., Proc., Vol. 63, pp. 707-709, June 1966.
20. Popovics, S. Contribution to the Prediction of Consistency. RILEM Bull. No. 20, pp. 91-95, Paris, Sept. 1963.
21. Powers, T. C. Topics in Concrete Technology 2. Analysis of Plastic Concrete Mixtures. Jour. PCA Res. and Development Labs., Vol. 6, No. 2, pp. 48-64, May 1964.
22. Powers, T. C. Studies of Workability of Concrete. ACI Jour., Vol. 28, pp. 419-448, Feb. 1932.
23. Grim, R. E. Applied Clay Mineralogy. McGraw-Hill, New York, 1962.
24. Martin, T. R. Adsorbed Water on Clay: A Review. Clays and Clay Minerals, Vol. 9. Proc. Ninth Natl. Conf. on Clays and Clay Minerals, pp. 28-70, Pergamon Press, New York, 1962.
25. Mielenz, R. C. Concrete as a Modern Material. In Modern Materials (B. W. Gonser, editor). Academic Press, New York and London, pp. 259-363, 1965.
26. Tanaka, T., Gotoh, K., and Shinohara, K. Cohesion of Fine Particles. Minerals Processing, Vol. 7, No. 3, pp. 32-33, March 1966.
27. Bombled, I. P., and Kalvenes, O. Comportement rhéologique des pâtes, mortiers et bétons: mesure, évolution, influence de certains parametres (Rheological Behavior of Pastes, Mortars and Concretes: Measurement, Evolution, Influence of Certain Parameters). Revue de Matériaux de Construction, "Ciments et Bétons," No. 617, Feb. 1967.
28. Náray-Szabó, I., and Szuk, G. The Determination of the Optimal Water-Cement Ratio of Concrete by Electrical Means. Acta Geologica, Vol. 3, No. 1-3. pp. 105-114, Budapest, 1955.
29. Prior, M. E., and Adams, A. B. Introduction to Producers' Paper on Water-Reducing Admixtures and Set-Retarding Admixtures for Concrete. Symposium on Effect of Water-Reducing Admixtures and Set-Retarding Admixtures on Properties of Concrete. ASTM STP 266, pp. 170-179, June 1960.
30. Popovics, S. What Should an Engineer Know About the Nature of Admixtures. To be published by "Concrete," London.

31. Newman, K. Concrete Systems. In Composite Materials (L. Holliday, editor). Elsevier Publishing Co., Amsterdam/London/NewYork, pp. 336-452, 1966.
32. Powers, T. C. The Nature of Concrete. Significance of Tests and Properties of Concrete and Concrete Making Materials. ASTM STP 169-A, pp. 61-72, Philadelphia, 1966.
33. Powers, T. C. Some Analytical Aspects of Fresh Concrete, 1 and 2. Cement Lime and Gravel, Vol. 41, No. 2 and 3, pp. 29-36, and 67-73, Feb. and March 1966.
34. Powers, T. C. Some Physical Aspects of the Hydration of Portland Cement. Jour. PCA Res. and Development Labs., Vol. 3, No. 1, pp. 47-56, Jan. 1961.
35. Copeland, L. E., and Schulz, E. G. Electron Optical Investigation of the Hydration Products of Calcium Silicates and Portland Cement. Jour. PCA Res. and Development Labs., Vol. 4, No. 1, pp. 2-12, Jan. 1962.
36. Komlos, K. K otazke sledovania viskoznych vlastnosti cementovich kasi, malt a betonov (A Contribution to the Viscous Properties of Cement Pastes, Mortars and Concretes). Stavebnicky Casopis, Vol. 9, No. 4, pp. 214-233, Bratislava, 1961.
37. Nessim, A. A., and Wajda, R. L. The Rheology of Cement Pastes and Fresh Mortars. Mag. of Conc. Res., Vol. 17, No. 51, pp. 59-68, June 1965.
38. Orr, C., Jr., and Blocker, H. G. The Viscosity of Suspensions of Spheres. Jour. of Colloid Sci., Vol. 10, No. 1, pp. 24-28, Feb. 1955.
39. Plowman, J. M. The Workability of Vibrated Concrete. Mag. of Conc. Res., Vol. 6, No. 15, pp. 127-130, London, March 1954.
40. Plowman, J. M. Measuring the Workability of Concrete. The Engineer, pp. 1007-1009, London, June 17, 1960.
41. Powers, T. C. The Bleeding of Portland Cement Paste, Mortar and Concrete. ACI Jour., Proc., Vol. 35, pp. 465-480, June 1939.
42. Steinour, Harold H. Further Studies of the Bleeding of Portland Cement Paste. Bull. 4, Research Laboratory of the Portland Cement Association, 1945.
43. Papers on Soils, 1959 Meetings. ASTM STP 254, Philadelphia, 1960.
44. Abrams, D. A. Design of Concrete Mixtures. Bull. No. 1. Lewis Institute, Chicago, 1918.
45. Talbot, A. N., and Richart, F. E. The Strength of Concrete, Its Relation to the Cement, Aggregates and Water. Bull. No. 137, Eng. Expt. Sta., Univ. of Illinois, 1923.
46. Young, R. B. Some Theoretical Studies on Proportioning Concrete by the Method of Surface Area of Aggregates. Proc., ASTM, Vol. 19, Part II, Philadelphia, 1919.
47. Solvey, R. O. Neue rationelle Betonerzeungung. Springer Verlag, Wien, p. 4, 1949.
48. Arrhenius, S. Über die innere Reibung verdünnter wasseriger Lösungen (The Internal Friction of Diluted Water-Solutions). Zeitschrift für Physikalische Chemie, Vol. 1, No. 6, pp. 285-298, July 1887.
49. L'Hermite, R. The Rheology of Fresh Concrete and Vibration (Translated from the French). Cement and Conc. Assoc., Translation No. 9, London.
50. Papadakis, M. Rhéology des suspensions de ciment (Rheology of Cement Suspensions). Revue des Matériaux de Construction, No. 476, May 1955.
51. Bombled, J. P. Rhéology du béton frais (Rheology of Fresh Concrete). Revue des Materiaux de Construction, "Ciments et Bétons," No. 591, Dec. 1964.
52. Mohan, D., and Goel, R. K. One-Point Method of Determining Liquid Limit. Soil Sci., Vol. 91, No. 2, pp. 100-102, Feb. 1961.

Chemical Expansion of Fresh Concrete By Use of Aluminum Powder And Its Effect on Strength

DON A. LINGER, Eric H. Wang Civil Engineering Research Facility, University of New Mexico

Laboratory evaluation of the expansion of fresh concrete resulting from the addition of powdered aluminum is described. The results show that the restraining of the fresh concrete is as important as the amount of expansion agent in determining the compressive strength of the hardened material.

It was found that the increase in volume due to the expansion agent reduces the strength of the hardened mixture, whereas confinement of the fresh mixture to retard expansion restores the strength according to the final volume achieved by the fresh mixture. Results are presented that show the change in volume that can be expected for various amounts of expansion agent and the effect of uniaxial confining pressure on the expansion and strength.

•IN the past three decades, many researchers have experimented with expansive cements in connection with the need for compensating for shrinkage (1, 2, 3, 4, 5). Chemical agents were added that caused the concrete to expand, but in many cases the expansion occurred after a long period of time, even months after placement (1). The expansion studied in this investigation is a rapid volumetric increase occurring before the hardening of the concrete. The use of aluminum powder in grouting has stimulated research on the expansion of fresh concrete and its effect on the mechanical properties of the hardened material (3, 4).

This study is an attempt to extend knowledge of the physical properties of a sand-cement grout which expands, prior to setting, as a result of the addition of powdered aluminum as the expansive agent. Addition of the aluminum causes a chemical reaction that produces hydrogen gas. As more gas is evolved, the grout expands and the air content increases. The major portion of the expansion occurred within 90 minutes of the mixing period. The rate of expansion is a function of the amount and fineness of the aluminum added, as well as of the temperature during the setting of the concrete (2). In this research only one type of aluminum powder was used and conditions during setting were the same for all specimens; therefore, it was assumed that the expansion characteristics were a direct function of amount of aluminum added.

The objective of this study was to evaluate the compressive strength and expansion characteristics of an expansive grout. This was studied by the addition of various amounts of the expansion agent, and the evaluation of the pressures exerted by the fresh concrete during expansion and formation of the compressive test specimens.

After hardening, the specimens were moist-cured for 28 days and then tested for their compressive strength. The relationships between strength, percentage of aluminum powder, and restraining pressures were then evaluated. These relationships give an indication of the amount of expansion that can be expected from the fresh con-

Paper sponsored by Committee on Mechanical Properties of Concrete and presented at the 47th Annual Meeting.

crete or the pressure exerted when it expands, and also what compressive strength can be expected when the grout sets with and without this pressure.

These relationships were found to be fairly well defined between the limits of aluminum added. Aluminum was added in the amount of 0.01, 0.025, 0.05, and 0.07 percent by weight of cement. At the outset, a preliminary study was made in which aluminum was added in the amount of 1 and 10 percent. The 1 percent aluminum expanded on the order of 30 percent to 40 percent and did not set; the 10 percent completely disintegrated while undergoing the setting process. The aluminum percentages vary over a wide range for this particular type of expansive grout and give a good idea of the percentages that should be used in future work.

LABORATORY PROCEDURE

Specimen Fabrication

At the outset of the experiment a preliminary study was made in which different amounts of aluminum powder were added to get an approximation of the maximum expansion to be expected for each percentage of aluminum used. This was done so that the final height of the specimens in the study could be made as close as possible to the necessary 12 in. used in the standard 6- by 12-in. cylinder, for the various amounts of expansion agent and restraining conditions.

The compressive tests on the hardened material were performed with 6- by 12-in. cylinders, cured, cast, and tested according to ASTM standards. The restraining effect was produced by placing weights on circular plates which were on the surface of the fresh concrete in the cylinders. The volumetric change was determined by the movement of the circular plates. Therefore, it should be noted that the volume change and restraining pressures were uniaxial in concept, thus approximating the condition of grouting reinforcing bars or filling voids in hardened media with grout.

Concrete Mix Design

The concrete mixture, which was a sand-cement grout, was proportioned as follows:

1. Cement-sand ratio, 1:2 by weight;
2. Water-cement ratio, 0.50 by weight; and
3. Aluminum powder added in amounts of 0.01, 0.025, 0.050, and 0.070 percent by weight of cement.

The cement was Type I portland cement. The powdered aluminum was that type used as a base for No. 1 Cres-Lite paint, produced by Crescent Bronze Powder Co., Los Angeles, California.

Itemized Laboratory Procedure

1. For each percent of aluminum (0.025, 0.050, 0.070), eight cylinders were cast (two for each confining condition). Two cylinders each at 0 and 0.01 percent aluminum were also cast. (These were left unrestrained in the cylinders, and only 28-day strength was recorded.)
2. The sand-cement-aluminum-water mixes were placed in 6- by 12-in. cylinders so that the final expanded length of the grout would be approximately 12 in.
3. Circular plates $5\frac{7}{8}$ in. in diameter and $\frac{1}{2}$ in. in thickness were placed on top of the grout in the cylinders.
4. Weights of 5, 20, and 85 lb were placed on the circular plates to attain restraining pressures of 0.177, 0.708, and 3.01 psi respectively. The standard cylinders were left unconfined by plates.
5. Measurements of change in length of the cylinders were made until expansion was negligible. The measurements were made by recording the movement of the restraining plates on the surface of the fresh concrete in the cylinder molds. Readings were taken on two sides of the cylinder and averaged.
6. The cylinders were left in the laboratory with weights still intact for 24 hours.

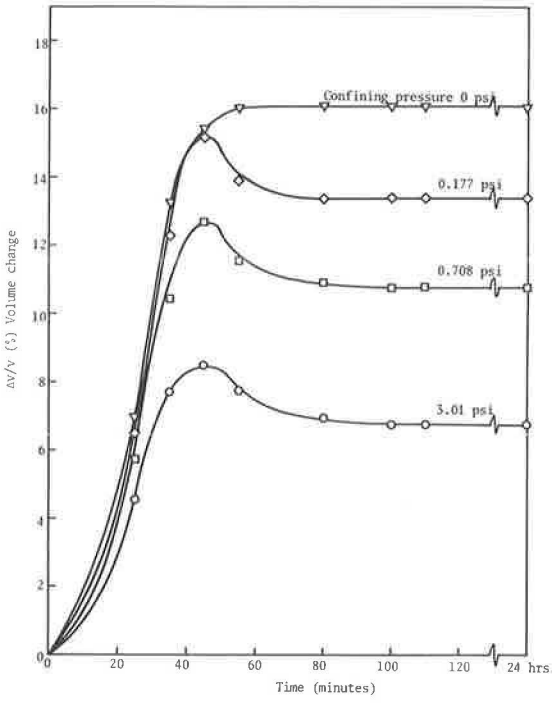

Figure 1. Volumetric expansion of concrete with 0.025 percent aluminum.

the strength of the hardened specimens. The loaded or restrained cylinders for the 0.050 and 0.070 percent aluminum reached a maximum expansion, then dropped and leveled off at some lesser expansion. The 0.025 percent aluminum mixture does not show this characteristic. This is the result of the 0.050 and 0.070 percent aluminum cylinders exerting enough expansion pressure in the production of gases to achieve a release pressure which, when it occurred, resulted in a decrease in volume at the end of the gas-producing cycle; however, the mixes with 0.025 percent aluminum did not produce the gas pressure necessary to achieve this action.

Figures 4, 5, and 6 relate the maximum expansion, confining load, and 28-day compressive strength. Figure 4 shows that the maximum volumetric expansion vs confining load curve might be extrapolated and the resulting x-axis intercept would represent the forces required to restrain the cylinders to zero

7. A final reading was taken, and the weights were removed after the 24-hour period.

8. The cylinders were moist-cured for 28 days.

9. The cylinders were then capped and loaded to failure in the compression machine.

RESULTS AND DISCUSSION

In this research emphasis was placed on the effect aluminum has on the mechanical properties of concrete. The curves of percentage of volumetric expansion vs time (Figs. 1, 2, 3) for the three percentages of aluminum show that, as might be expected, the rate of expansion and final amount of expansion increase as the percent of aluminum increases.

Also as expected, the increase in aluminum powder results in a marked decrease in strength. However, a restraining pressure applied to the cylinders during the setting period results in a reduction in the rate and total expansion, and an increase in

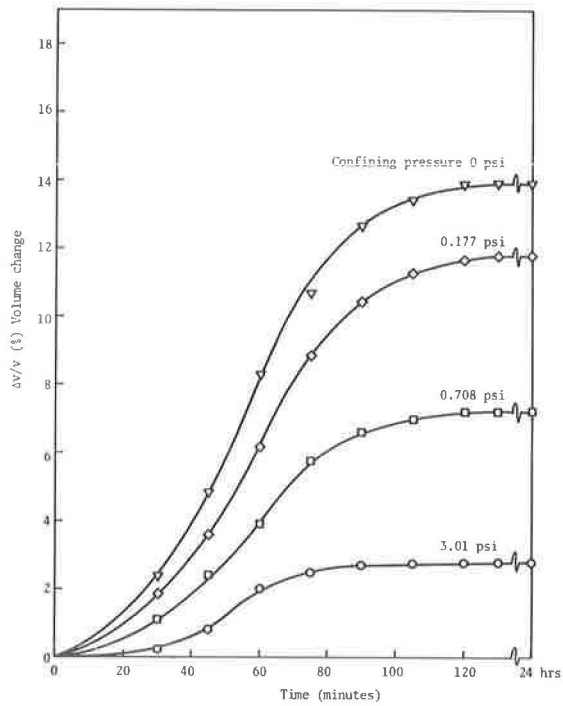

Figure 2. Volumetric expansion of concrete with 0.050 percent aluminum.

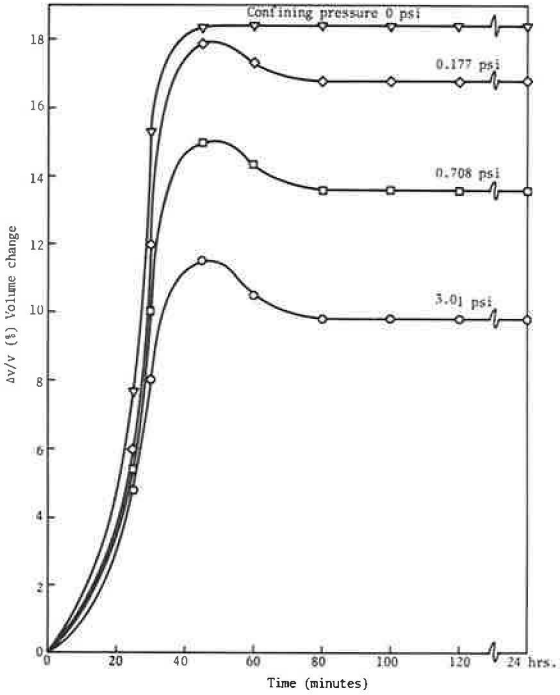

Figure 3. Volumetric expansion of concrete with 0.070 percent aluminum.

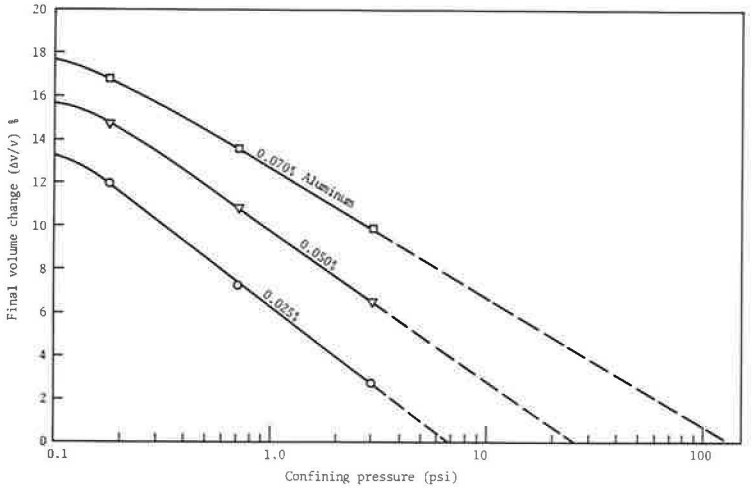

Figure 4. Effect of confining pressure on final volumetric expansion.

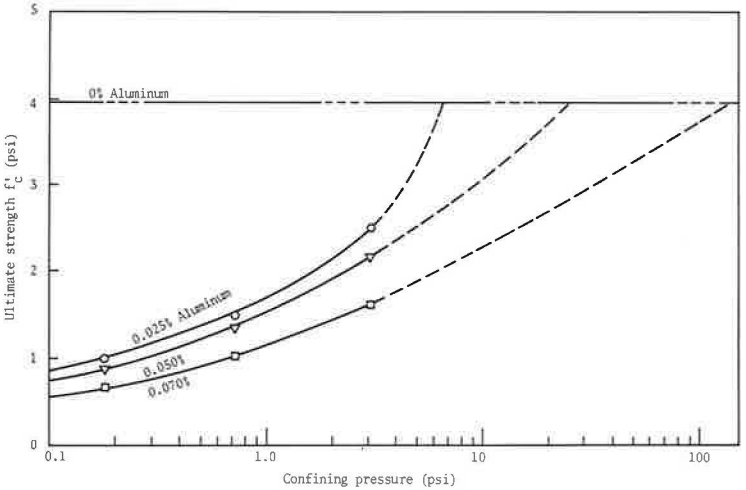

Figure 5. Effect of confining pressure on 28-day strength.

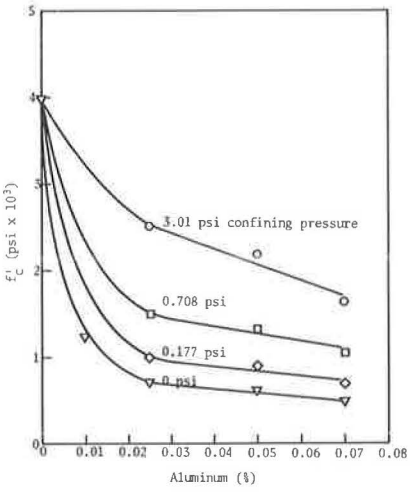

Figure 6. Relationship between compressive strength and percent aluminum.

expansion. Similarly, the strength vs confining pressure curves in Figure 5 can be extended to the pressures predicted from Figure 4, which are necessary to fully restrain the concrete from expanding. The resulting extrapolated compressive strengths are all close to the average f'_c value (3,980 psi) for the cylinders cast with no aluminum present. Although the accuracy of the extrapolation is questionable, the increase in compressive strength resulting from larger confining pressures is apparent. This indicates that the loss in strength acquired by the presence of aluminum is due only to the additional voids caused by the increase of air content. That is, if the cylinders containing aluminum were not allowed to expand they would have the same compressive strength as cylinders in which no aluminum was added. This implies that the chemical reaction that takes place has no other effect on the mix than the production of hydrogen gas, which is entrapped and thereby increases the air content and volume. This is also indicated by the curve of percentage of aluminum vs 28-day strength (Fig. 6). It is seen that as the confining load on the cylinders increases the compressive strength approaches 3,980 psi.

Figure 4 shows that after a minimal restraining load has been applied to the concrete, the volumetric expansion is inversely proportional to the log of the confining load. Figure 6 indicates that a marked decrease in strength occurs up to 0.02 percent aluminum, after which addition of aluminum has less effect on the strength.

CONCLUSIONS

The results of this study show the increase in volume that can be expected with the addition of various amounts of powdered aluminum to a concrete mixture. The expansion is the result of gas produced by the mixture and occurs prior to hardening. The expansion is difficult to control for little or no confining pressure, and the results

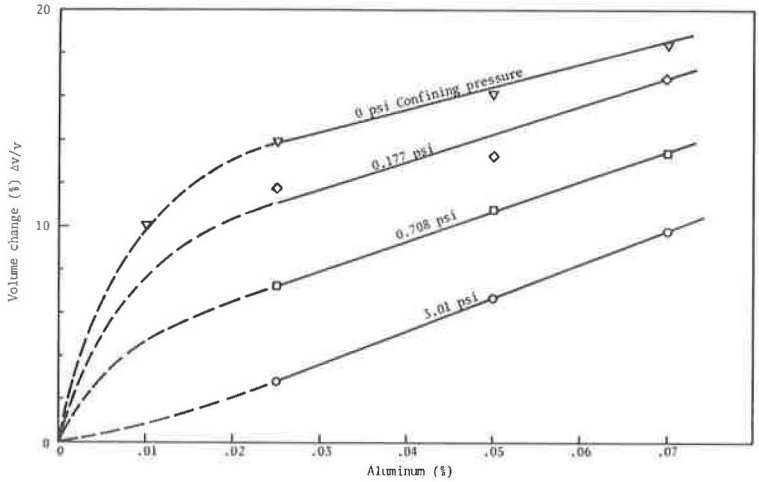

Figure 7. Relationship between aluminum content and volume change.

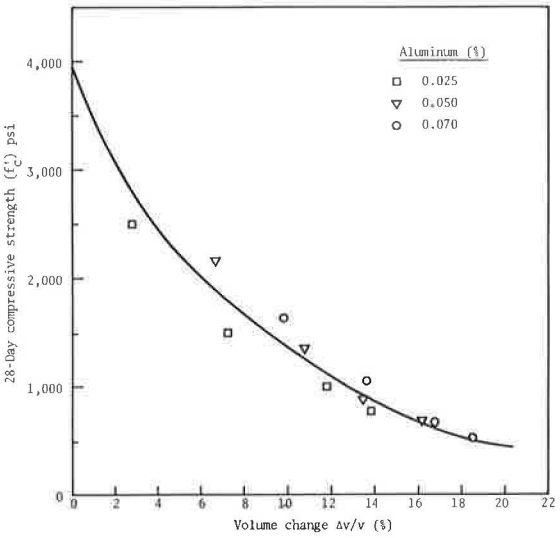

Figure 8. Relationship between strength and volume of voids.

in general indicate that the increase in volume is very sensitive to small quantities of the expansion agent. However, the expansion becomes linear for large quantities of the expansion agent (Fig. 7). Figure 7 also indicates that the expansion is easily controlled with the addition of very small confining pressures. Therefore, controlled expansion is possible with the magnitude and control depending upon the amount of the expansion agent and the confining pressures.

Although there is a significant reduction in strength occurring with the addition of the expansion agent, this reduction is dependent upon the final volume change of the fresh mixture. This is shown in Figure 8, in which the strength data are related to the volume change of the fresh mixture, irrespective of the confined condition or percentage of the expansion agent. This reduction in strength indicates the adverse effect of voids in concrete on the compressive strength. Moreover, since the reduction in strength is the result of the formation of voids during the expansion, the final 28-day strength of the hardened mixture can be predicted if the final volume change is known.

REFERENCES

1. Monfore, G. E. Properties of Expansive Cement Made With Portland Cement, Gypsum, and Calcium Aluminate Cement. Jour. PCA Res. and Dev. Labs., Vol. 6, No. 2, pp. 2-9, May 1964.
2. Investigation of Shrinkage-Resistant Grout Mixtures. U. S. Army Engineer Waterways Experiment Station, Tech. Rept. No. 6-607, Aug. 1962.
3. Menzel, Carl A. Some Factors Influencing the Strength of Concrete Containing Admixtures of Powdered Aluminum. Jour. ACI (Proc.), Vol. 39, pp. 165-184, Jan. 1943.
4. Shideler, J. J. The Use of Aluminum Powder to Produce Nonsettling Concrete. Report No. C-192, Bureau of Reclamation Engineering Laboratories, Sept. 1942.
5. ACI Committee 212. Admixtures for Concrete. Jour. ACI (Proc.), Vol. 51, pp. 113-146, Oct. 1954.

Pavement Thickness Measurement Using Ultrasonic Pulses

MATTHEW J. GOLIS, The Ohio State University

A pulse-echo type of ultrasonic pavement thickness measuring system is described. The system's performance on newly constructed concrete pavements is reviewed. Recommendations for future system development are made along with design criteria for advanced versions of the present system.

The thickness measurements are based on ultrasonic pulse transit time measurements in pavements of known sound velocity. Accuracies of ±2 percent in better than half of the measurements taken were obtained during a testing program involving more than 350 measurements. Results were verified by core measurements made by the testing laboratory of the Ohio Department of Highways. This accuracy was attained through the use of large-area ultrasonic transmitters, high pulse powers, and high frequencies of operation (300 kHz).

During the evaluation program it was found that an assumed constant velocity of propagation over a finite area of pavement did not seriously impair the test results. Once velocity information was obtained for a given section of highway, it was found reasonably safe to consider that the velocity remained the same for considerable distances around the specific velocity measurement site.

•THE thickness gage described uses ultrasonic pulse techniques to measure thickness of portland cement concrete, in place, in highways. The need for accurate, nondestructive means of pavement thickness measurement is well known to highway engineers and contractors as well as to state and national agencies supporting highway construction and maintenance. Thus, it is not detailed here.

Efforts to develop ultrasonic methods for highly accurate (±2 percent) measurement of portland cement concrete thicknesses during the past 20 years have been generally unsuccessful in the United States and in other countries. Significant advancements were reported by Jones (1), Bradfield (2), and Muenow (3), but in all cases it was found that accuracies better than ±5 percent were very difficult if not impossible to obtain.

Two of the critical basic difficulties that have been encountered include (a) the relatively coarse-grained aggregates within the concrete that scatter, reflect, and severely attenuate high-frequency sound waves; and (b) the surface roughness (particularly of bottom surfaces on gravel or other subbase structures) that tends to destroy coherent ultrasonic reflections from these surfaces.

The pavement thickness measurement program described was specifically designed to compensate for these known difficulties through the use of novel transducer designs. The unusual features of the final design were specifically:

1. The use of unusually high ultrasonic power levels to compensate for signal attenuation in concrete due to the presence of coarse aggregate.
2. The use of large-diameter transducers that permitted averaging of bottom surface roughness.

Paper sponsored by Committee on Mechanical Properties of Concrete and presented at the 47th Annual Meeting.

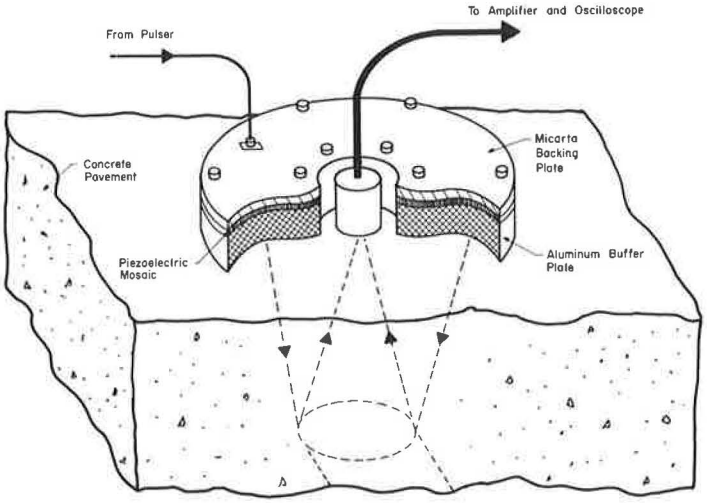

Figure 1. Functional drawing of the OSU/ODH Pavement Thickness Gage.

3. The use of high-frequency receiver systems to permit signal identification through wave shape observation.

By using these techniques, high-frequency operation for improved resolution of bottom surface location was obtained. The details of the gage are reviewed in the following discussions of theory and practice.

THEORY OF PAVEMENT THICKNESS GAGE OPERATION

The OSU/ODH Pavement Thickness Gage* measures pavement thicknesses by monitoring the amount of time it takes an ultrasonic pulse to travel down through the concrete and back again. The distance the sound travels is related to the transit time and sound velocity by the expression:

$$d = 2T = Vt \qquad (1)$$

where

d = distance traveled (in.),
T = pavement thickness = d/2 (in.),
V = velocity of sound propagation (in./sec), and
t = transit time (sec).

Figure 1 shows the organization of the system.

Once the transit time is measured, then the thickness can be readily calculated, given the speed of sound for the material. For example, a pavement 9 in. thick having a sound velocity of 144,000 in./sec (12,000 ft/sec) would have a measured transit time $125(10)^{-6}$ sec (125 μsec). A pavement 10 in. thick with a velocity of 16,000 ft/sec would have a transit time of 104 μsec. Thus, the technique for measuring the pavement thickness is to establish the sound velocity for the local pavement material and to measure the transit times throughout the area.

The sound velocity can be obtained in various ways. One way is to take a transit time measurement for a pulse traveling down and back through the pavement. When

*The abbreviations represent the developmental and sponsoring agencies, i.e., Ohio State University and Ohio Department of Highways, in conjunction with the Bureau of Public Roads.

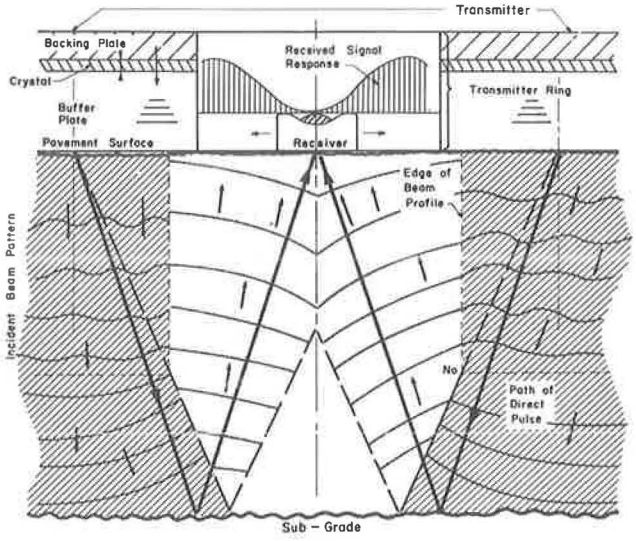

Figure 2. Schematic drawing of the sound field in the vicinity of the OSU/ODH Pavement Thickness Gage.

this time is compared to a core's length taken from the same area, the velocity can be computed by using Eq. 1. Although this technique was the one used for the initial evaluation of the OSU/ODH Pavement Thickness Gage on sections of Interstate highway systems near Columbus, Ohio, it was found that thickness accuracies within ±2 percent could be attained by assuming an average velocity throughout the 351 tests.

Due to the geometry of the transmitter and the location of the receiver, the ultrasonic beam path is not straight down and back, but rather follows a triangular path. The actually measured transit times are therefore slightly longer than those obtained by a pulse traveling straight down and back. This extra time corresponds to approximately 4 percent of the total transit time for the geometry used. However, it was found that an effective velocity could be used to describe the thickness of the pavement (effective signifying the velocity needed to describe the actual thickness given the measured transit time). Errors introduced by using this procedure are less than 1 percent in 8- to 10-in. pavements.

The Ultrasonic System

The detection system of the pavement thickness gage is based on the divergence of sound from an ultrasonic radiator. As a pulse of ultrasound propagates down through the concrete, it spreads out. Thus, the receiver, located at the geometrical center of the large transmitting radiator, obtains a useable signal. Although the large-area transmitter tends to concentrate the sound beam for better conservation of ultrasonic power density, it does not destroy the effect of the receiver's capability. Figure 2 shows the approximate ultrasonic profile of the sound beam within the concrete developed by such a large-area transmitter arrangement.

Note that in this configuration the receiver is physically removed from the transmitter area. This permits better isolation of transmitter noise from signal returns. The transmitter is in the form of a disc with a hole in its center for positioning of the receiver. Most effective was a transmitter with an outside diameter of 16 in. and an inside diameter of 4 in. The ultrasonic sound generator is a mosaic piezoelectric radiator composed of 20 segments of a modified barium titanate material (Channelite 300). It has a characteristic thickness resonance frequency of 400 kHz to which it responds when excited with an electrical impulse. When mounted in the assembly, this drops to about 300 kHz. The mosaic, although composed of several independent elements, responds acoustically as a single radiator when excited electrically. This capability has permitted high-energy ultrasonic pulses distributed over a broad area to be introduced into pavement materials for thickness gaging purposes.

The aluminum buffer plate located between the piezoelectric element and the pavement serves as a 3-in. protective layer between the ceramic-like element and the highly abrasive concrete surface. Due to multiple reflections within the buffer plate, a second transmitted pulse approximately 30 μsec behind the initial pulse is transmitted and often assists in identifying the bottom reflection signals in the presence of excessive background noise. The buffer plate also supplies sufficient weight to the assembly to assure good contact between the transmitter assembly and the pavement material.

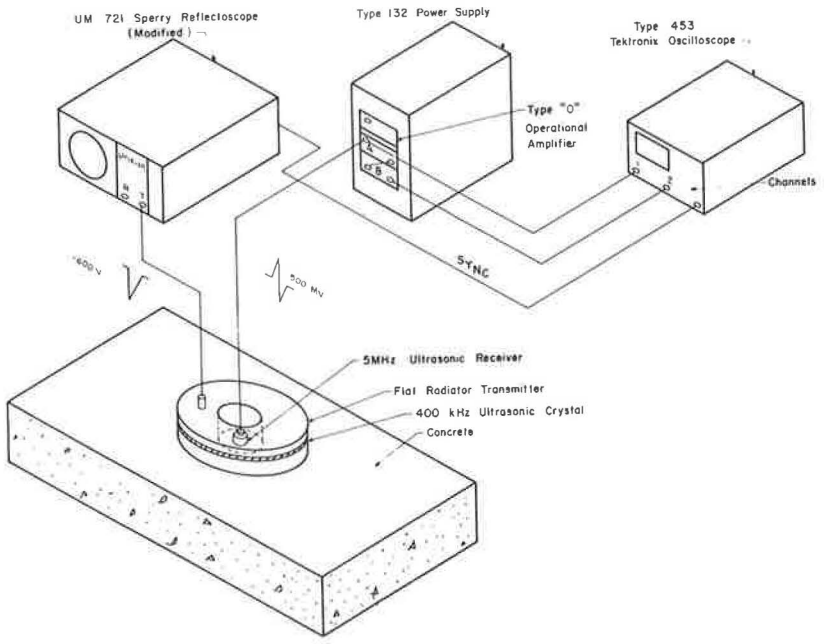

Figure 3. Block diagram of the OSU/ODH Pavement Thickness Gage.

Mathematical analysis of the theoretical sound fields showed that the main or central lobe of the transmitter (and therefore reflected) energy covers a radius of $^{3}/_{4}$ in. Thus, in order to maximize the response of the system, the receiver transducer was especially designed to be at least 1.5 in. in diameter. Experimental evidence showed an increase in receiver output of 10 times that previously available using smaller area receivers.

When a receiver is frequency-matched to an ultrasonic oncoming signal, the true shape of the received pulse is usually lost, although the output is high. Since it was found that bottom surface signals were identified by a characteristically high-frequency pulse, a receiving transducer with natural resonant frequency well above the frequency of the incoming signal was chosen. For a 200 to 400 kHz input signal, a 5 MHz receiver was found to be best. Thus, the special purpose receiver is 1.5 in. in diameter with a natural thickness resonance of 5 MHz.

The Electrical System

The electrical system used in the Pavement Thickness Gage is representative of a typical A-scan configuration often found in ultrasonic nondestructive testing. This type of presentation displays ultrasonic signal amplitude as a function of time. A block diagram of the system is shown in Figure 3. The unit providing the timing as well as the pulse excitation for the ultrasonic system is a typical multivibrator and thyratron pulser configuration. Signals corresponding to reflected ultrasonic pulses from the bottom surface of the concrete are detected by the high-frequency receiver located at the geometrical center of the transmitter. The received pulses may be amplified and/or modified in the operational amplifier and are then displayed by the type 453 Tektronix oscilloscope. The pulser unit is capable of delivering 600 volts at 75 amperes to a 5 ohm capacitive load for 1 μsec pulses.

Placement of the receiver probe in direct contact with the transmitter yields pulses of 6 volts peak amplitude. Since the receiver probe has a surface area equal to $^{1}/_{75}$ that of the transmitter's area, the drop from 600 volts excitation to 6 volts reception is to be expected. The wave-shape of this received signal is shown in Figure 4.

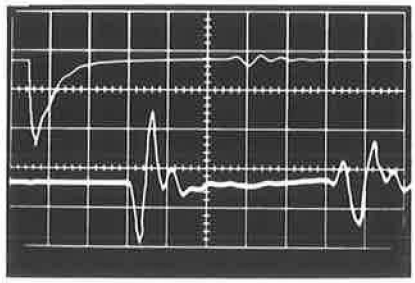

Figure 4. Excitation and received signals through 3-in. aluminum buffer plates.

Use of Operational Amplifiers

The operational amplifier is usually used for direct amplification of low-level signals. When identification of the received pulse is difficult, differentiation and amplification of the input signal may supply a uniquely clear indication of the received pulse. This follows since identification of the received signals is done through observation of a signal with a steeper slope than that of the background noise.

Under good conditions, the signal to noise (S/N) ratio was of the order of 2. When these signals are differentiated, their derivative is substantially larger than that of the background. The S/N ratio is improved to 5 or better.

FUNCTIONAL OPERATION OF THE OSU/ODH PAVEMENT THICKNESS GAGE

The usual technique of testing uses two operators. One operator handles the transmitter and receiver on the road surface while the other records the transit times measured from the oscilloscope. The transmitter and receiver are ultrasonically coupled to the pavement by a bentonite and water paste. The receiver in the center of the transmitter is moved about to assist the recorder in absolutely identifying the reflected signal. When a reflection from the base of the pavement is clearly visible on the oscilloscope, its exact transit time is recorded.

In most cases, the oscilloscope has sufficient signal amplification capabilities to give a satisfactory presentation of signal shape on the screen. For those cases in which the received signal is weak and very close to the background noise level, additional amplification can be supplied by an external operational amplifier.

The positive identification of the bottom surface reflected pulse (in the presence of background noise) is made by recognizing its unique high-frequency shape. Noise signals received in addition to the bottom surface signals are mostly at a frequency of about 10 kHz as opposed to the 300 to 400 kHz bottom reflection signal.

Signal Identification

Signal identification and interpretation are relatively simple using the Pavement Thickness Gage. Nearly every signal will show a low-frequency pulse at and around the time corresponding to the bottom thickness. Superimposed on the low-frequency waveform is the characteristic high-frequency bottom echo signal. The oscilloscope adds these two signals. The result is shown in Figure 5.

The labels in Figure 5 refer to the main factor for consideration in the pavement depth calculation:

T_{tt} = total transit time from pulse initiation to received signal display.

T_d = delay time, or the length of time necessary for the pulse to traverse the aluminum block of the transmitter.

T_{ta} = actual transit time, or the length of time necessary for the pulse to traverse the distance from pavement top surface to bottom surface and back to the receiver.

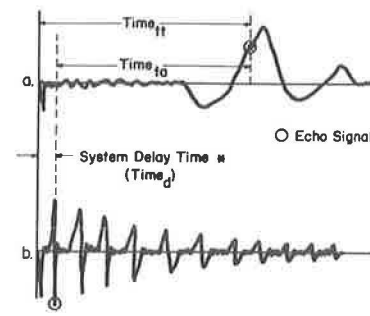

Figure 5. Oscilloscope display of satisfactory received signal.

There are occasions when the waveform completely "covers" the high-frequency echo pulse. In such instances, the signal display has the appearance of Figure 6a. In this situation the operator can usually improve the signal and make it more intelligible

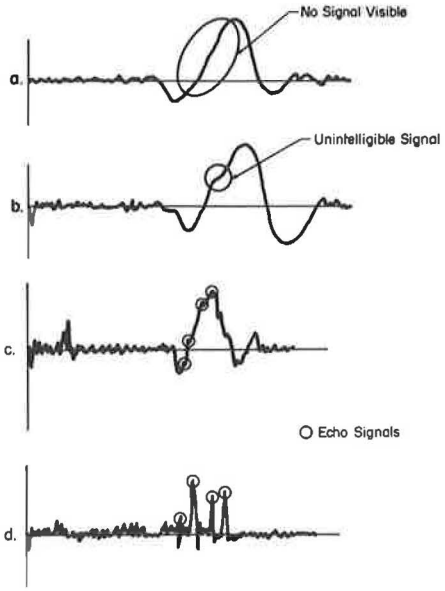

Figure 6. Oscilloscope display of unsatisfactory but informative signals.

by repositioning the transmitter and/or receiver. He can also make significant improvements by recoupling the transducer assemblies to the pavement. Figure 6b is another example of the same kind of signal; in this case the echo is visible, but not intelligible—i.e., the operator is unable to determine with precision where the peak of the pulse lies on the waveform.

Ordinarily, the signals obtained in the field vary between the types of signals shown in Figures 5a, 6a, and 6b. Whenever signals of types 5a and 6b are present, clarity and intelligibility can be improved by repositioning either the transmitter or receiver, or both, or by improving the coupling of the transducers to the pavement.

Sometimes a waveform such as shown in Figure 6c and 6d is displayed on the oscilloscope. Each of the points is an intelligible signal. The signal generally indicates to the operator either honeycomb on the bottom surface or lack of bonding at the subbase surface. Because this type of trace indicates a flaw in the integrity of the concrete, it is useful as a nondestructive test of pavement; but in order to establish a true depth, a good bottom echo must be obtained. In other words, when a signal trace of this type is encountered, the presence of the honeycomb can be recorded, but the transducer must be moved until a good echo is obtained before the true depth can be determined.

The Pavement Thickness Gage was evaluated by taking a series of transit times over a given testing area of pavement from which a single core had been removed. The core was used to find the effective velocity for the region. With this velocity information, it was possible to predict the thickness of remaining locations through the region by measuring the corresponding transit times.

A program of field testing was carried out using the flat-radiator version of the Pavement Thickness Gage during the late autumn of 1966 and the summer of 1967. The program that was followed and the results of the testing are outlined next.

FIELD TESTING PROGRAM

The field testing program was conducted on several unopened sections of Interstate highway throughout Ohio. Thickness measurements were taken both at sites which had been previously cored by the ODH testing laboratory personnel and at untested locations. Velocity data were initially obtained from transit time readings taken at a site which was subsequently cored and measured. With this information as a basis for testing, the remaining core locations were tested ultrasonically.

Core site locations were made available to the testing program through the cooperation of the ODH. During ultrasonic testing, the center of the area measured was marked with paint to assist the core driller in locating the site and to assure that identical test sites were used.

General Observations

Seven thickness measurements using ultrasonic techniques could usually be taken each hour. The present ODH rate is 20 cores a day, plus the time in the laboratory required to mechanically measure the cores.

There were some sections of pavement where the reflected signal was consistently hard to read. In these areas, the operating rate could be cut to only four measurements an hour plus extra care required in setting up equipment. Under favorable

TABLE 1

Site	No. of Comparisons	Avg. Thickness* ODH	Avg. Thickness* OSU	Discrepancy* ODH-OSU	% Accuracy (ODH/OSU) x 100
IR 75	45	9.12	9.03	-0.09	100.97
IR 77	52	9.02	8.95	-0.07	100.82
IR 70	60	9.08	9.47	+0.39	95.88
IR 270	86	9.09	9.20	+0.11	98.80
IR 275	20	9.02	9.40	+0.38	95.95
US 30	23	9.07	8.96	-0.11	101.22
IR 70	42	9.04	9.08	+0.04	99.55
	328	9.07	9.17	+0.10	98.90

* Thickness and discrepancy in inches.

operating conditions, rates of ten or more measurements an hour were maintained. For the hard-to-read regions, subsequent testing has revealed that these conditions are indications of such pavement characteristics as honeycombing, cracking, and general degradation of the pavement.

TEST RESULTS

More than 350 thickness measurements were taken by using the Pavement Thickness Gage during 1967. Of these, 150 were taken after the core had been cut. ODH and the ultrasonically measured pavement thicknesses agreed with ±2 percent in better than half of the measurements taken. For 9-in. pavement, ±2 percent is equivalent to an average difference of ±0.18 in. Perfect agreement between the two measuring systems occurred in 17 percent of the total readings. Comparative results of typical job sites and a major sampling of the type of results obtained by the Pavement Thickness Gage are given in Table 1. Accuracies on a job basis were mostly within 2 percent with two exceptions. The averages of the total program are within 1 percent, even though the two exceptions are both positive deviations.

The variances are attributed primarily to (a) the inherent averaging procedures used in the tests, (b) the differences in operating personnel, and (c) the acoustic characteristics of the pavement materials. Since the effective velocities used and the measure-

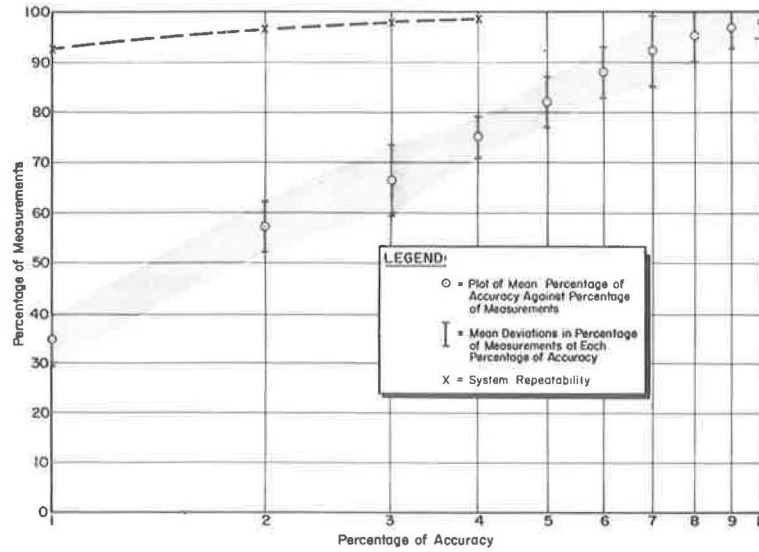

Figure 7. Average accuracy of the OSU/ODH Pavement Thickness Gage.

ments are based on the averaging of the ultrasonic pulse transit times representing pulse paths distributed over a 16-in. diameter ring, the ultrasonic gage is measuring an area four times the size of the ODH core. Thus, all of the variations within this larger area are also being compared to the core measurement. The figures also represent the training of three people in the operation of the equipment and all of the potential variations inherent in such a procedure. The velocity of sound in concrete throughout a given paving job was assumed constant. This was found true over modest segments of highway.

Figure 7 shows the results of the first 351 measurements made using the Pavement Thickness Gage. It shows the agreement of the OSU and ODH measurements for the total testing program and the duplication uncertainty found in the system. The results are expressed as the percentage of times the results fell within the specified ratios. For example, 35 percent of the measurements taken were within 1 percent of the ODH readings. The upper curve represents the variations found in merely trying to duplicate previous readings and is considered the best possible system performance.

Some of the more gross disagreements between OSU and ODH readings have been attributed to the varying characteristics of the concrete pavements. By examining cores that were cut at the same site at which ultrasonic gage results were incorrect, obvious problems in the concrete have been observed. Large pebbles, air pockets or uncommonly rough bottoms have usually been prevalent in these sample cores. Some of the cores inspected were found to be so bad that they broke apart during the coring process. Pavements in such condition can make the thickness gage ineffective for thickness measurement, but then it signals the presence of poor concrete by its noticeable lack of detectable signal. No effects were found present due to steel reinforcing rods in the pavements.

The degree of reproducibility of results and the system's inherent uncertainty are also shown in Figure 7. This curve was made from the normalized results of four separate readings taken at one site. The readings were normalized with respect to their average value. This is equivalent to the consistency of the system at a single core site. Figure 7, therefore, shows the highest performance which can be expected from this system. The graph indicates that about 92 percent of the results are consistent within ± 1 percent.

A similar plot constructed from data taken from typical mechanical tests made by the ODH testing laboratory has the same shape and value distributions. For the data obtained from ODH, 91 percent consistency was obtained within the ± 1 percent deviation, indicating that the ultrasonic system's reproducibility is equivalent to that of the mechanical testing procedure.

While poorly laid concrete does make the taking of measurements difficult, it is not the only road problem. Initial investigations showed that ridges in the top surface of the pavement of $\frac{1}{8}$ in. or more produce sufficient distortion in the incident and received pulses to make interpretation difficult. In addition, when the ridges are this deep it is difficult to maintain sufficient ultrasonic coupling between the transmitter and the road surface.

Measurements have been made on samples ranging from $7\frac{1}{2}$ to 10 in. thick. When samples are smooth on both sides, this range doubles. Beyond approximately 15 in., the signal attenuation is too large for reception of detectable signals. Below 5 in., the signal distortion makes interpretation of return signals impossible in many cases. These limits should cause little problem in highway testing, however, since the average pavement thickness of 9 in. is well covered.

Nominal velocity values were calculated from the transit time measurements resulting from field tests. The distributions of ultrasonic agreements with ODH measurements were observed using progressively higher velocities until an optimum in agreement was reached. The velocity yielding the optimum correlation was taken as the characteristic velocity for that section of pavement. The velocities obtained thus were later used to predict the pavement thickness throughout each given job.

In general, the gage characteristics can be summarized as follows:

1. It supplies data on pavement thickness with accuracies of ±2 percent or better in more than half of the recorded measurements.

2. It is operable in the field as well as in the laboratory.
3. It can detect high-frequency sound pulses in concrete throughout a range of 5 to 15 in.
4. It requires operator interpretation of signal readout and data reductions.
5. It is nondestructive to the pavement.

CONCLUSIONS

The OSU/ODH Pavement Thickness Gage has demonstrated its ability to measure pavement thickness. Because this ultrasonic device is nondestructive during each test, significantly larger numbers of thickness samplings can be made when evaluating the thickness of pavements. The accuracy of the system is attributed to the use of high-frequency and high-power transducer elements. The program has demonstrated the extreme usefulness of ultrasonic technology to the highway industry.

REFERENCES

1. Jones, R. Measurement of the Thickness of Concrete Pavements by Dynamic Methods: A Survey of the Difficulties. Mag. of Conc. Res., Vol. 7, No. 1, pp. 31-34, Jan. 1949.
2. Bradfield, G., and Woodroffe, E. P. H. Determination of Thickness of Concrete Pavements Using Mechanical Waves. Rept. No. Phys./U5, Great Britain, Dept. of Sci. and Indus. Res., National Physical Laboratory, Feb. 1953.
3. Muenow, R. A. A Sonic Method to Determine Pavement Thickness. Jour. PCA Res. and Development Labs., Vol. 5, No. 3, pp. 8-21, Sept. 1963, Research Department Bull. No. 163.

Earth-Resistivity Tests Applied as a Rapid, Nondestructive Procedure for Determining Thickness of Concrete Pavements

R. WOODWARD MOORE, Office of Research and Development,
U. S. Bureau of Public Roads

•EARTH-RESISTIVITY tests have long been employed as a rapid procedure for making subsurface explorations dealing with such highway construction problems as slope design, foundation conditions, landslide investigations, and location of construction materials. Equipment for making such tests has been built or purchased by 39 states and Puerto Rico. In a continuing search for rapid, nondestructive test procedures for use in conjunction with or in lieu of currently used destructive tests, the U. S. Bureau of Public Roads has adapted the electrical resistivity test to determine the thickness of concrete pavements.

This test involves measuring the resistance to the passage of an electric current through the selected medium. The test is made by using four electrodes equally spaced in a line on the surface of the material being tested (see Appendix). The nature of the test is such that the effective depth (penetration of the applied current) can be varied and controlled by the spacing of the four electrodes as the test progresses; i. e., the effective depth is equal to the electrode spacing for a particular setting of the electrodes. Thus, when testing a concrete pavement the electrode system may be spaced at a 1- or 2-in. spacing for the initial readings of current and potential change, and the system expanded in 1-in. increments for successive readings extending to a total depth of 3 to 6 in. below the bottom of the pavement. Four small plastic tubes, plugged with stiff clay and filled with a saturated solution of copper sulfate into which a copper wire is inserted, are used in the test (Appendix, Fig. A-3). The clay, with the help of a slight wetting of the concrete surface, provides a suitable contact for the electrical circuits with the pavement surface.

A concrete pavement has a resistivity characteristic that usually differs from that of the underlying soil or base layers. When plotting resistivity against electrode spacing or depth, a change in resistivity is normally encountered in the base layer that will produce a recognizable trend in the curve towards a higher or lower resistivity, signifying the presence of the underlying material. Using the Moore Cumulative Curve Method of depth determination (briefly described in the Appendix), it is possible to draw straight-line portions of the cumulative curve to intersect in the vicinity of the trend appearing in the field curve (dashed-line curve in several figures), the depth at which the intersection is obtained being equated to the thickness of the layer under test.

The results of some 150 tests, made on both unreinforced and reinforced concrete slabs and on bridge decks, have been good. A linear regression analysis of resistivity measurements and direct pavement thickness measurements made at 68 locations gave the following results: (a) an average thickness ($\bar{Y}$) of 9. 55 in., (b) a standard error of estimate (S_E) of 0. 226 in., and (c) a coefficient of variation of 2. 36 percent. However, it should be emphasized that some experience in the use of the test and the method of analyzing the test data may be required for the best results. Much more testing is needed to determine the effectiveness of the proposed test procedure under all field

Paper sponsored by Committee on Mechanical Properties of Concrete.

conditions, varying concrete mix, air entrainment and water-cement ratio of the concrete, and base-course design.

Steel reinforcing produces recognizable changes that do not interfere with thickness measurements and, in fact, offers a good possibility that the effects could be utilized to measure the depth of the steel. More work is needed, however, to determine whether a dependable depth determination is possible without some prior knowledge of the position of the steel beneath a test center.

TESTS ON CONCRETE ROADWAY PAVEMENT

Figure 1 shows the data plotted for a test made on a 9-in. plain (nonreinforced) concrete pavement recently placed in the repair of a section of the George Washington Memorial Parkway in Northern Virginia. The gradual but definite uptrend appearing in the dashed-line curve at a depth of 8.0 in. is the basis for choosing the intersection of the solid straight lines at 8.85 in. in the cumulative curve as an indication of the thickness of the slab. The thickness established by level rod readings made on the top of the compacted sand and gravel base and on the finished concrete surface is shown along the base of the graph. The relatively close check between the results of the resistivity test and the directly measured thickness is not uncommon. For 31 locations on this project, the variation of the resistivity thickness determinations from the linear regression equation ranged from +0.35 to -0.57 in., with an average deviation of 0.141 in. (1.52 percent). When it is considered that a much larger sample is involved to some degree in the resistivity test (an area 45 in. by 18 in. for a 9-in. slab) in contrast to the 4-sq in. area of the level rod base, any small percentage difference becomes even less significant.

The foregoing results and other tests made on plain concrete slabs appear to confirm the test procedure for use under such conditions. Other variables, such as the presence of steel reinforcing and the age of the structure, remain to be evaluated. Figure 2 shows the results of a test made on a slab, nominally of 9-in. thickness, with reinforcing steel in the upper third of the slab. This test was one of 34 made on Interstate 66 in Rosslyn, Virginia, just prior to its being opened for traffic. The sharp downtrend in the early part of the dashed-line curve of Figure 2 was produced by the effect of the steel reinforcing present in the upper third of the pavement. As noted earlier, this effect on the measured resistivity may have significance in obtaining information concerning the position of the steel. However, it should be emphasized that the primary purpose of the several tests under discussion was to obtain overall thickness measurements of the concrete slabs involved. Mention of the possible location of the position of the reinforcing steel in subsequent paragraphs is made in a discussion of the extra downtrends appearing in the curves and to suggest, perhaps, that further consideration should be given to this possible use of the test. Further discussion of this possibility is made in a later section.

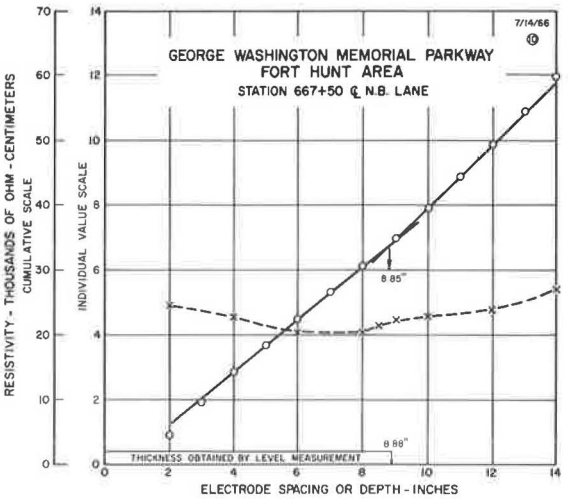

Figure 1. Earth-resistivity test over plain concrete slab to obtain thickness—sand and gravel base.

The presence of the steel makes it possible for abnormally high current densities, not controlled by the resistance of the concrete mass, to be recorded, which results in the rapid drop in resistivity shown in the curve of Figure 2. This effect continues as the test progresses through the pavement and becomes more pronounced as the effective depth reaches and passes the contact between the pavement and the underlying base material (cement-treated sand and gravel). The

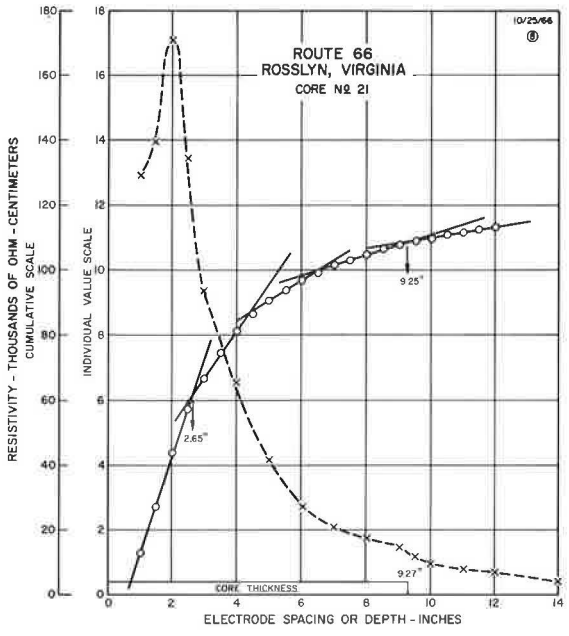

Figure 2. Earth-resistivity test over reinforced concrete roadway slab to obtain thickness—cement-treated base.

test was not carried to a sufficient depth to permit an attempt to determine the thickness of the base course. The thickness obtained by a measured core is shown at the base of the graph. The good agreement between measured thickness (9. 27 in.) and resistivity results (9. 25 in.) suggests that a very uniform bottom condition exists throughout the 5- to 6-sq-ft area of the slab likely to influence the test to some degree. The two intersections obtained in the cumulative curve (solid-line curve) at 4. 35 in. and 6. 5 in. were discounted as not being significant in the analysis, in the absence of additional recognizable trends in the dashed-line curve. Similar extraneous intersections also were obtained in the cumulative curves of Figures 4 and 5. The higher initial resistivity values of Figure 2, when compared to those involving the first 8 in. in the preceding graph for the test on plain concrete, which averaged 4, 500 ohm-cms, are likely a result of air entrainment, effect of curing compound, and differences in the composition of the concrete used on the two construction projects.

Although the time required to make the 16 separate determinations of resistivity used to plot the dashed-line curve in Figure 2 was 15 to 20 minutes, further simplification of apparatus and field techniques could reduce the required time to only a 5- to 10-minute period. For example, if there was no interest in attempting to determine the depth of the reinforcing steel, resistivity readings beginning with an electrode spacing of 7 in. (corresponding to an initial depth of 7 in.) and continuing only to a 12-in. depth would produce sufficient data to permit a satisfactory thickness determination for a 9-in. concrete slab. Also, assuming no interest in a measurement of natural potentials, sometimes an important adjunct to resistivity measurements, alternating current apparatus could be devised to permit a direct reading of resistivity that could speed up an analysis of the data obtained.

Figure 3 shows resistivity data for a test made on a 5-in.-thick slab with steel mesh reinforcing at the midpoint. This slab, recently placed on the

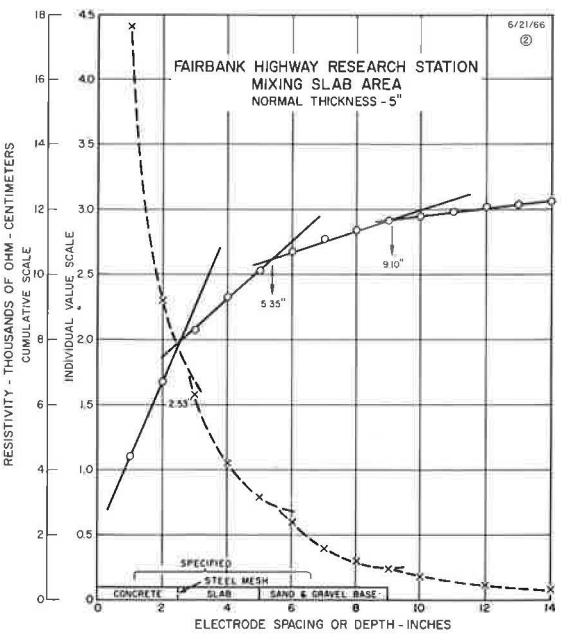

Figure 3. Earth-resistivity test over reinforced concrete slab—5-in. thickness on sand and gravel base.

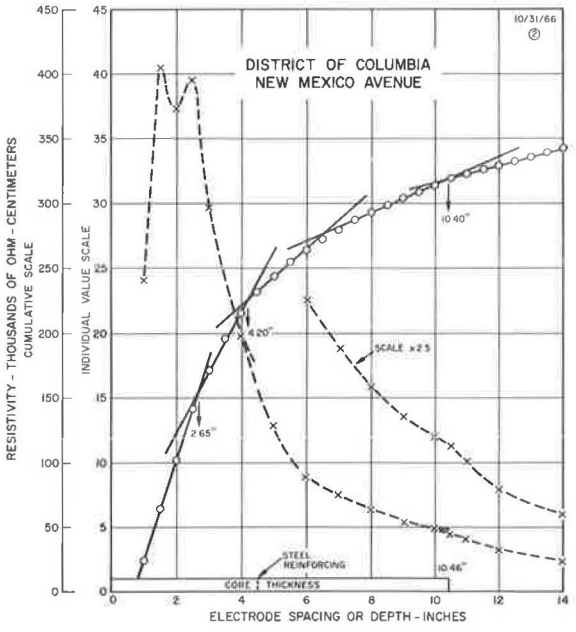

Figure 4. Earth-resistivity test over reinforced concrete roadway slab—10-in. thickness.

grounds of the Fairbank Highway Research Station, provided a 30- by 40-ft working surface for mixing large masses of soil for laboratory use; thickness control could have been rather casual. The changes indicated at depths of 2. 53, 5. 35, and 9. 10 in. appear to be associated with the depth of the steel reinforcing, the bottom of the concrete slab, and the bottom of the 4-in. layer of granular base beneath the slab, respectively. The results of seven tests made on this slab gave average depth values of 2. 65, 5.16, and 9.21 in. for the three changes shown in Figure 3. No direct measurements of the slab thickness, position of the reinforcing steel, and the base-course thickness have been made at this location.

Figure 4 shows data for tests made on a reinforced concrete pavement subjected to 3 or 4 years of traffic on New Mexico Avenue in Washington, D. C. The changes shown at depths of 4. 20 and 10. 40 in. have apparently located the position of the steel and the bottom of the slab. The length of the core obtained at this location was 10. 46 in. The average thickness for four tests made on the project was 0. 1875 in. lower than that found by coring. The change showing at a depth of 2. 65 in. in Figure 4 is likely associated with near-surface changes in the concrete.

Tests made on both plain and reinforced concrete roadway slabs in service for 17 years produced resistivity-thickness curves of substantially the same character as those shown in the figures. Apparently, corrosion of the reinforcing steel, if present, does not cause a significant change in the recorded effect of the steel on the measured values of the resistivity.

TESTS ON CONCRETE BRIDGE SLABS

It would seem that a much closer control of steel positioning and slab thickness is possible when placing concrete bridge slabs and, consequently, there would be less need for a nondestructive thickness test for such structures. The resistivity test should be considered as a possible rapid, nondestructive test procedure, however, if coring is done or if there is a definite need to locate the steel reinforcing after construction. Figure 5 shows

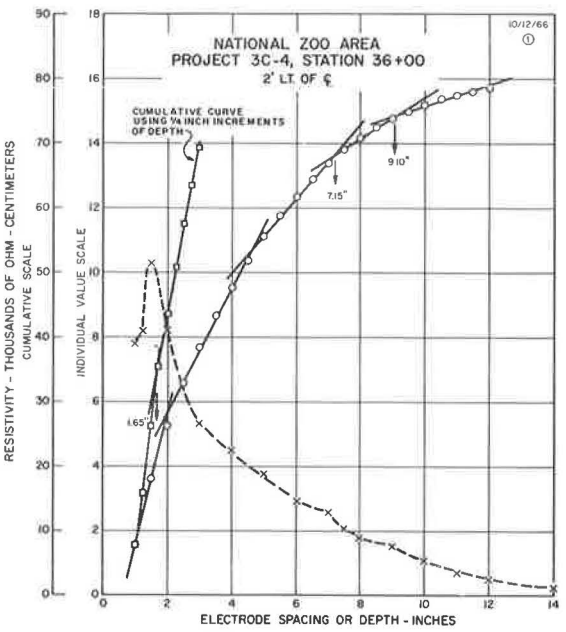

Figure 5. Earth-resistivity test over top slab of box girder bridge structure—9-in. section.

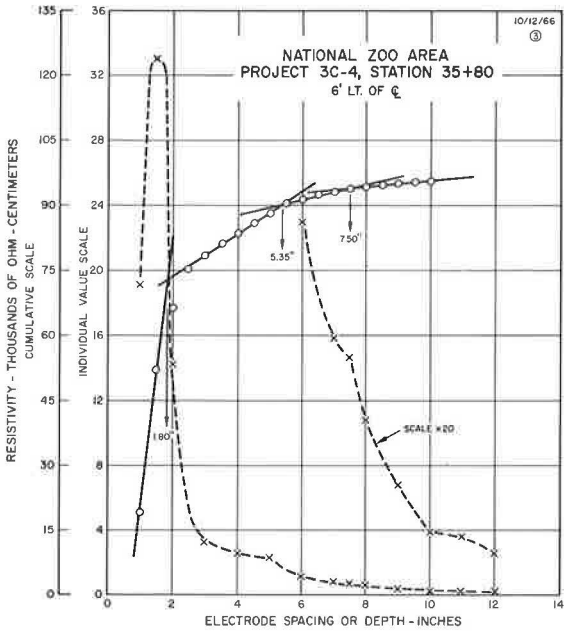

Figure 6. Earth-resistivity test over top slab of box girder bridge structure—7-in. section.

data obtained on the top deck of a concrete box girder bridge in the District of Columbia. The changes indicated at depths of 1.65 and 7.15 in. are associated with the steel reinforcing cage. The data for the first 3 in. of depth in the curve of Figure 5 were replotted in a cumulative relation using a ¼-in. increment of depth to obtain the change shown at a depth of 1.65 in. The final change at 9.10 in. represents the bottom of the slab. Similar results were obtained elsewhere on the bridge where a 9-in. thickness was specified. The average depths obtained for the seven tests made were 1.80, 7.25, and 9.14 in.

Figure 6 shows the results of a test made over a section of the bridge deck having a 7-in. specified thickness. The probable position of the steel in this instance was indicated at depths of 1.80 and 5.35 in., the slab thickness being 7.50 in. The results from 10 tests made over the 7-in. - thick areas gave average values for these three depths of 1.86, 5.21, and 7.04 in. respectively.

LOCATION OF REINFORCING STEEL

An extra dividend of resistivity tests to obtain slab thickness may be the location of the reinforcing steel in reinforced concrete pavements. If this is a current problem in post-construction evaluation of reinforced concrete pavements, the resistivity test should certainly be given a thorough trial for such use. In Figure 2, the change at a depth of 2.65 in. was produced by steel mesh found at a depth of 3.0 in. in the core. In Figure 3, the change found at a depth of 2.53 in. showed good agreement with the design depth of 2.50 in. shown on the graph. In Figure 4, the change at a depth of 4.2 in. compares fairly well with the depth of 4.5 in. found for the steel in the core removed from the pavement. No direct check for steel positioning was made for the test locations involved in Figures 5 and 6. The specifications indicated a 1½-in. cover for the steel near to the surface of the bridge slab and a 1.0-in. cover at the bottom. The average cover indicated by the 17 tests made on the bridge was 1.83 in. at the top and 1.86 in. at the bottom.

Some error could be introduced into the measurements made to locate the steel, however, due to the size and location of the steel bars with respect to the test center. Random positioning of the center of the electrode system between two bars rather than directly above a bar could possibly affect the depth indicated. Also, it is not known whether the effect produced on the resistivity measurements corresponds to the top of the steel or its center. Obviously, much trial testing over known steel positioning will be necessary before the effect of such possible sources of error can be fully evaluated.

CONCLUSION

Although the results obtained thus far in attempting to measure the thickness of concrete by use of the earth-resistivity test suggest a very useful application of the test, there is need for further trial tests. These, preferably, should be made by personnel of several state highway departments scattered throughout the country, to thoroughly evaluate the test procedure for conditions existing in differing geologic areas and

to involve a wide variety of concrete mixes and base layer construction. Because many states already have equiment useful for such research, new HPR research programs might readily be actuated. Such testing should not overlook the possible use of the measurements to locate the steel in reinforced concrete slabs.

Appendix

The earth-resistivity test involves the introduction of a direct or alternative electric current into the material being tested and the measurement of its resistance to passage of the current. Four electrodes are used and are spaced equal distances apart and on a straight line (Fig. A-1). The current passing through the material between electrodes C_1 and C_2 is measured, and the potential drop between electrodes P_1 and P_2 is recorded. The resistivity for a 1-cc volume is computed by using the formula $P = 2\pi A E/I$, in which A is the electrode spacing in centimeters, E the potential drop in volts, and I the current in amperes flowing between C_1 and C_2. The assumption is made that equipotential hemispheres or bowls with a radius A are established around each current electrode (C_1 and C_2). Every point on the surface of a hemisphere has the same potential. By placing the potential electrodes P_1 and P_2 at points on the surface where these hemispheres intersect the ground surface, it is possible to measure a potential drop that applies equally well at a depth A below the surface. As the electrode system is expanded to involve greater depth, the bottom of the hemispherical zones may involve a layer of differing electrical resistivity, which produces a trend towards lower or higher resistivity and gives an indication of depth to the layer producing the resistivity change. The resistivity values are plotted against electrode spacing or depth as shown by the dashed-line curve of Figure A-2. The solid-line curve of Figure A-2 is a cumulative plotting of the data for the dashed-line curve in which the first point is the same value as the first point of the dashed-line curve plotted to a condensed scale, the second point is the sum of the resistivities for the first and second points, the third point is the sum of the resistivities for the first three points, etc. Using a constant increment of depth throughout, i. e., 3 ft, the solid-line curve constitutes a graphical integration of the dashed-line curve. Straight lines drawn through the plotted points in the vicinity of a trend in the dashed-line curve intersect to give the depth to the subsurface layer producing the trend.

Figure A-3 shows a typical miniature resistivity test in progress. The small plastic tubes are plugged with stiff clay and filled with a solution of copper sulfate in which copper wires are immersed. The clay permits a very slow movement of the copper sulfate solution to the concrete surface and, along with a slight wetting of the concrete surface, provides for good electrical contact. These electrodes are spaced at a 1- or 2-in. initial setting, when testing thing layered structures such as concrete pavements, and are expanded with 1- or 2-in. increments to carry the test to a depth some 3 to 6 in. below the bottom of the layer being investigated. Generally, with respect to concrete pavements, there is a measurable difference in resistivity between concrete and the materials normally used in the base layers.

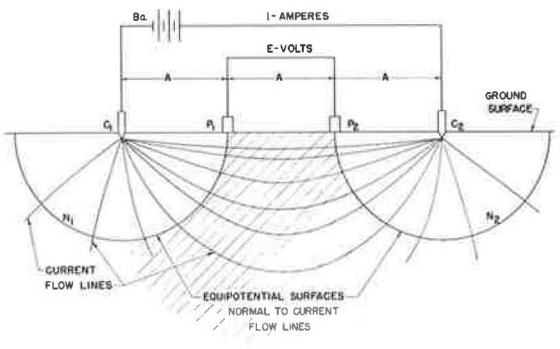

Figure A-1. Equipotential bowls assumed beneath current electrodes when making earth-resistivity tests.

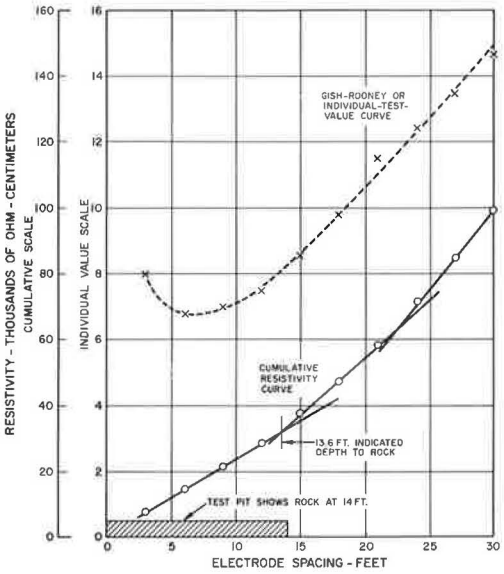

Figure A-2. Typical resistivity data and method of analysis using the cumulative resistivity curve.

Figure A-3. Typical miniature resistivity test in progress on concrete pavement.